

**TECHNICAL DEVELOPMENT REPORT NO. 367**

**The CAA Directional Localizer**

**FOR LIMITED DISTRIBUTION**

**by**

**Samuel E. Taggart  
Oliver J. DeZoute  
Walter M. Ehler**

**Electronics Division**

**August 1958**

**1616**

**FEDERAL AVIATION AGENCY  
TECHNICAL DEVELOPMENT CENTER  
INDIANAPOLIS, INDIANA**

**FEDERAL AVIATION AGENCY**

**E. R. Quesada, Administrator**

**D. M. Stuart, Director, Technical Development Center**

**This is a technical information report and does not  
necessarily represent FAA policy in all respects.**

## THE CAA DIRECTIONAL LOCALIZER

### SUMMARY

A localizer is that portion of the CAA instrument landing system which provides lateral guidance to an aircraft approaching a given runway. The directional localizer is used where a conventional localizer is not satisfactory. This report describes the results obtained with two experimental directional localizer installations developed at the Technical Development Center at Weir Cook Municipal Airport, Indianapolis, Indiana. A directional localizer antenna system consists of two parts: (1) a very directive array which provides course information a few degrees to each side of the extended centerline of a given runway, and (2) a clearance array which provides bearing or clearance information at all other azimuths. A slotted waveguide operating in the  $TE_{01}$  mode comprises the very directional portion of the antenna system. The first installation employed a waveguide 200 feet in length with  $3\frac{1}{4}$  vertical slots spaced 71 inches apart in the front face of the guide. The second installation utilized a 117-foot waveguide with 18 active vertical slots in its front face. The same clearance array, consisting of an 8-loop localizer array placed 50 feet to the rear of the waveguide, was used with both directional localizers. Tests were made throughout the localizer band 108 to 112 Mc.

The effectiveness of the waveguide in reducing course bends was clearly demonstrated in ground and flight tests. Tests were conducted to determine the effects of reflecting objects in front of the localizer between  $2.8^\circ$  and  $25^\circ$ . An appreciable reduction in "siting error" was demonstrated in favor of the directional localizer. A large reflecting screen, placed 200 feet to the rear of the clearance array and oriented so as to produce large bends along the course when the clearance array only was operated, caused negligible bends when the directional localizer was placed in operation. The effect of temperature on the stability of three types of coaxial transmission line was investigated. A tuneup procedure for the antenna system is described.

### INTRODUCTION

Although the eight-loop localizer now in use at many airports has been improved over a period of years and is satisfactory in most cases, there are locations where nearby hangars or other large reflecting surfaces cause bends in the course. At these locations, special techniques are required.

Several large-aperture antenna systems have been developed which will provide straight courses at difficult sites.

Three types, namely, a parabolic reflector, a linear array, and a 105-foot slotted waveguide, were described in earlier reports.<sup>1,2</sup> Of these, the slotted waveguide appeared to show the most promise for use on the Federal Airways. The factors considered in adopting the slotted waveguide were: (1) simplicity of the feed system, (2) stability of course width and position, (3) a high degree of bend reduction, (4) a minimum of polarization error, and (5) ease of fabrication. This report describes two experimental directional localizers, using slotted waveguides, which demonstrate these features.

### THE 200-FOOT WAVEGUIDE

#### Description.

When the directional localizer experiments were initiated in September 1947, current standards for localizers required a nominal course width of  $5^\circ$ . Theoretical considerations of the slotted waveguide antenna<sup>1</sup> indicated that an aperture of 200 feet would place the major lobes of the sideband patterns at approximately  $2.5^\circ$  on either side of the course and thereby provide the maximum usable sharpness of course under existing localizer standards. A very high degree of bend reduction also would result. A slotted waveguide 200 feet long was fabricated of galvanized sheet iron, using standard sheet-metal practices in its construction. Thirty-four slots spaced 71 inches apart ( $169^\circ$  at 109.9 Mc) were provided, all of which were employed except the one nearest each end of the waveguide. The centers of the slots were 52 inches above the ground as measured at the middle of the front face of the waveguide. Figure 1 is a view of the 200-foot slotted waveguide. An 8-loop clearance array was located approximately 50 feet behind the waveguide. The loops of the clearance array were mounted one-half wavelength above a wire mesh screen laid on the floor of the antenna shelter. The plane of the loops was 20 inches above the centers of the slots of the waveguide. Figure 2 is a block diagram of the mechanically modulated directional localizer.

#### Adjustment.

The calculated aperture field distribution of the 200-foot waveguide was based on the binomial difference series<sup>1</sup> of 160 terms. Only the center 32 terms were used. The series represented a compromise between relative amplitude of the minor and major lobes of the sideband pattern and the angular spacing between the major lobes. A greater number of terms in

<sup>1</sup>Chester B. Watts, Jr., "Some Considerations of Wide Aperture Localizer Antennas," Technical Development Report No. 155, January 1952.

<sup>2</sup>Chester B. Watts, Jr., Samuel E. Taggart, and Kennard E. Voyles, "Development of a VHF Directional Localizer," Technical Development Report No. 183, May 1954.

the series would have resulted in a somewhat decreased angular spacing of the major lobes, but an increased amplitude of the minor lobes. A smaller number of terms in the series would have resulted in increased spacing of the major lobes, reduced amplitude of the minor lobes as compared to the major lobes, and increased difficulty in reading accurately the relative slot currents near the ends of the guide.

An improved radio-frequency (r-f) probe for exciting a slot was developed which caused only a few degrees variation in phase at its associated slot when the slot current was changed by probe adjustment.<sup>3</sup> The angles at which the probes were set, to obtain the desired current at each slot, were calculated after measuring the characteristics of one probe. All probes then were set accordingly. Indirect indication of the relative slot currents were obtained with the small r-f measuring device shown in Fig. 3. The theoretical and measured slot currents for carrier and sideband distribution are given in Figs. 4 and 5. Later tests indicated that the discrepancy between the theoretical and the measured patterns shown in Figs. 4 and 5 is due primarily to the change in guide wavelength caused by the individual slot excitation probes. No allowance for this effect was made when the angles at which the probes should be set were calculated. The result, as far as the field patterns were concerned, was much the same as if a smaller number of terms had been used in the binomial series, that is, the minor lobes were decreased and the angle between the two major lobes of the sideband patterns was increased. The carrier pattern also was made somewhat broader. Figure 6 shows the method used for supplying sideband and carrier power to the waveguide. Lines  $L_1$  and  $L_2$  each were originally 105-foot lengths of RG-17/U transmission line, and  $L_3$ ,  $L_4$ , and  $L_5$  each were  $0.158\lambda$  lengths of RG-8/U transmission line.  $L_6$ , also made of RG-8/U transmission line, was  $0.658\lambda$  long. Sideband power was fed to the bridge at the junction of  $L_3$  and  $L_4$ , and carrier power was supplied at the junction of  $L_5$  and  $L_6$ . The lines  $L_1$  and  $L_2$  were supported against the bottom of the waveguide and connected between the other two corners of the bridge and the 27-inch vertical whip antennas used to excite the waveguide. The measured voltage standing wave ratio (VSWR) at the input corners of the bridge was found to be approximately 10 to 1 before matching. After matching, the VSWR at each input of the bridge was reduced to less than 1.1 to 1.

#### Tie Line Stability.

After the waveguide was placed in operation and the course width had been set to  $5^\circ$  by changing the sideband power supplied to the guide as required, it was observed that the course width changed with a change in

<sup>3</sup>The slot probe used previously with a 105-foot waveguide consisted of a bent 1/4-inch brass rod. Slot current was controlled by changing the depth of penetration of the probe into the waveguide. This caused considerable change in r-f phase at the associated slot. The new design probe, which was used in the 200- and the 117-foot waveguides, also was bent, but was arranged to pivot about at a fixed point; therefore, the total length of probe inside the waveguide remained constant during adjustment of slot current.

temperature. It also was observed that the VSWR at the input corners of the r-f bridge feeding the guide changed with variation in ambient temperature. The cause of the variation in the VSWR at the input corners of the bridge, and indirectly, for the change in the course width, was found to be due to variation in the length of tie lines  $L_1$  and  $L_2$  shown in Fig. 6. Investigation showed that, as the ambient temperature increased, the electrical length of the tie lines decreased. A test of air dielectric transmission line showed that it possessed a positive temperature coefficient about one-fourth as great as that of RG-17/U line and about one-sixth as great as that of RG-8/U line. Tests demonstrated that by using a combination of lengths of air dielectric and RG-8/U line, the resultant electrical length of the combined lines could be maintained to a very close tolerance. These results are shown in Fig. 7. After the original tie lines were replaced with a combination of air dielectric line and RG-8/U line, the variation in VSWR with change in ambient temperature was reduced to a very low value. Some additional stability was gained by changing the lines  $L_3$ ,  $L_4$ ,  $L_5$ , and  $L_6$  (Fig. 6) to  $0.1\lambda$ ,  $0.1\lambda$ ,  $0.25\lambda$ , and  $0.75\lambda$ , respectively. These changes in length in conjunction with some adjustment of the lengths of  $L_1$  and  $L_2$  resulted in an unmatched VSWR of approximately 2.5 to 1 at each input of the bridge. Matching the lines resulted in a VSWR of less than 1.1 to 1 in the carrier and sideband feed lines.

#### Tests.

Flight tests were made to record clearance and the field strength patterns of the 200-foot waveguide and of the 8-loop clearance arrays. The field strength meter used was a Type BC-733 receiver modified to give essentially linear indication with variation in field strength. The receiver used in obtaining the recordings of cross-pointer deflection was a standard Collins' Model 51-R-2.

Figure 8A is a recording of the field pattern of the waveguide array when unmodulated power was supplied to the sideband input of the r-f bridge. Azimuth is measured in a clockwise direction from the extended centerline of the runway. Amplitude of the received signal is directly proportional to the recorder deflection. It will be noted that the ratio of amplitude of the major lobes to the minor lobes is greater than 15 to 1, at all azimuths except  $177^\circ$  and  $183^\circ$  where there are two small lobes whose amplitudes are approximately 10 per cent as great as the major lobes. The difference in amplitude of the two major lobes probably is due to difference in the theoretical and the actual slot currents. No attempt was made to equalize the two major lobes. The angle between the two major lobes is slightly less than  $8^\circ$ , whereas the calculated value was  $5^\circ$ . Better agreement between the theoretical and measured spacing of the major lobes would have been obtained if all slot currents had been set more closely to the theoretical values given in Fig. 5.

Figure 8B is a recording of the field pattern of the waveguide when unmodulated r-f was supplied to the carrier corner of the bridge feeding the guide. The minor lobes and the lobe to the rear of the waveguide are all less than 5 per cent of the main lobe. The half-power width of the main lobe is approximately  $6^\circ$ .

Figure 8C is a recording of the field pattern when separate unmodulated r-f voltages differing in frequency by 10 kc were supplied simultaneously to the carrier loops of the clearance array and to the carrier corner of the bridge feeding the guide. The large lobe near  $0^\circ$  represents the carrier of the waveguide array. There is no discontinuity or irregularity in the recorded pattern to indicate the exact point at which control of the field strength meter shifts from the carrier of the waveguide to the carrier of the clearance array. The ratio of the field strength of the carrier of the waveguide on course to the carrier of the clearance array is approximately 6 to 1. The minor lobes of the waveguide are completely masked by the clearance array.

Figure 9A is a recording of the course deviation indicator (CDI) current when the waveguide array only was operating as a localizer. The course width is  $4.5^\circ$  and the crossover is smooth. Numerous reversals and points of low clearance are present. There is a rear course which appears nearly normal with respect to width and smoothness of crossover.

Figure 9B is a recording of the CDI current made when the eight-loop clearance array only was operating. Here the crossover on the front and the rear courses is smooth and there are no points of low clearance. The front course arbitrarily was set to a width of  $5.2^\circ$ , which resulted in a rear course width of slightly less than  $4^\circ$ .

Figure 9C is a recording of the CDI current when both the waveguide and the clearance arrays were in operation. A comparison of Figs. 9B and 9C shows that there is no significant difference between the two. The front course width is only slightly less when the two arrays are operating simultaneously than when the clearance array only is operating. The clearance array does not control the receiver over the azimuth sector in which the carrier field strength of the waveguide is much greater than the carrier field strength of the clearance array.<sup>4</sup>

Ground tests of the installation were made at a distance of 5,000 feet using a Collins 51R2 receiver mounted in a truck. Readings were taken in mid-morning of the working day and again in the late afternoon. The equipment was turned off daily and over weekends, but was given a warmup period of 1 hour prior to the time observations were made. No adjustment was made to any part of the receiving equipment or the transmitting equipment during a 20-week period. The measured variations in course position and course width of the waveguide array, and of the clearance array operating separately and simultaneously, are shown in Figs. 10 and 11, and include all errors due to variation in the directional localizer installation, ground and weather conditions, and truck-mounted measuring equipment.

In Fig. 10, which is a bar graph of course position variation, it will be noted that the waveguide, operating by itself, showed a maximum total

<sup>4</sup>Chester B. Watts, Jr., op. cit.

variation in course position of plus or minus  $0.05^\circ$ . The clearance array, when it was operated by itself, showed a total variation of approximately plus or minus  $0.125^\circ$  course deviation during the same period. When the waveguide was operated in conjunction with the clearance array, the maximum total variation in course position was approximately plus or minus  $0.05^\circ$ . This indicates that the waveguide had predominant control of the course position.

The bar graph in Fig. 11 shows the variation in course width of the waveguide operating by itself, of the clearance array operating by itself, and of the two arrays operating simultaneously. The significant feature of this graph is the close correlation between the course width of the waveguide operating by itself and in conjunction with the clearance array. It will be noted that there is only random correlation between the variations in course width of the clearance array and of the waveguide array. This is further evidence that the waveguide controlled the course width in a narrow sector on each side of the course.

### THE 117-FOOT WAVEGUIDE

#### Description.

While the 200-foot waveguide provided excellent results, it was recognized that the degree of bend reduction which could be expected was more than would be necessary at the majority of airports where severe bends of the localizer course existed. After a careful study of the performance of the 200-foot and the 105-foot<sup>5</sup> waveguides, it was decided that a guide with an aperture of 117 feet with 20 slots should provide sufficient bend reduction. This reduction in aperture from 200 feet to 117 feet also should result in a substantial reduction in the initial cost of the waveguides.

Plans were drawn for a new waveguide having inside dimensions 117 feet long, 77 inches wide, and 40.75 inches high. The new waveguide was mounted on the same structure that was used for the previous model. The midpoints of the slots were 52 inches above ground at the middle of the waveguide, and the spacing between the waveguide slots and the clearance array was 50 feet. The clearance array was left unchanged. Figure 12 is a view of the 117-foot waveguide and the 8-loop clearance array.

Changes in construction of the new waveguide over the two earlier models included: (1) a sloped corrugated sheet metal roof which overhung the front face of the guide approximately one foot, (2) a Fiberglas cover over each of the 20 slots, (3) teflon spacers and mechanical stabilizers at each slot, (4) an improved access port at the center of the rear face of the guide, (5) rigid mounting arrangements for the excitation probes, (6) additional supporting members under the bottom of the guide, and (7) the soldering of all seams on the inside of the guide. An improved device for measuring relative slot currents also was developed. This device, with which a high degree of repeatability of readings was obtainable, is shown

<sup>5</sup>Chester B. Watts, Jr., op. cit.



in Fig. 13 set in position for use just under the sloping bottom of the Fiber-glas slot cover. In addition to the above changes in the waveguide, the mechanical modulation system used on the earlier directional localizers was replaced by electronic modulation in order to conform with standard Federal Airways localizer installations. Figure 14 is a block diagram of the electronically modulated directional localizer using the 117-foot waveguide.

In determining the relative slot currents for the sideband distribution of the 117-foot waveguide, the binomial difference series was employed where the number of terms equals 82. Only the 18 middle terms of this series were used. The theoretical and measured sideband slot currents are given in Fig. 15. The slot currents for the carrier distribution of the new waveguide are given in Fig. 16. It will be noted that there is considerably more variation between the theoretical and the measured values of the carrier distribution than there is between the same two curves of the sideband distribution. This is a normal situation in practice because the probes are adjusted as necessary to obtain, as closely as practicable, the theoretical sideband slot current distribution, and the resulting carrier slot current is accepted.

Figure 17 shows the theoretical sideband pattern of the 117-foot waveguide from  $0^\circ$  to  $16^\circ$  off the runway centerline and the sideband pattern of a conventional localizer plotted to the same slope in the direction of the runway centerline. A comparison of the two curves is indicative of the bend reduction obtained when using the slotted waveguide antenna instead of the conventional localizer antenna.

It will be noted that the amplitude of the minor lobes in the sideband pattern is approximately 6 per cent of the major lobe. The minor lobes could have been reduced to a lower value by using a smaller number of terms in the binomial series on which the sideband currents are based, but this would have resulted in a greater angular spacing of the two major lobes of the sideband field pattern, and the course, since it is determined by the waveguide, would have been further subject to the effect of reflecting objects. By operating the waveguide as a clipped binomial array, many of the advantages of an array with an aperture of 450 feet are obtained in the 117-foot waveguide.

The ratio of the amplitudes of the two curves shown in Fig. 17 is plotted in Fig. 18. This curve represents the ratios of the bend-producing energy of the two types of antenna operating singly over the azimuth shown. The abscissa may be defined as the bend reduction factor of the 117-foot waveguide array over the 8-loop clearance array.

#### Adjustment of the Waveguide and R-F Bridge.

The arrangement of r-f bridge and tie lines for the 117-foot waveguide was similar to that used on the 200-foot waveguide. See Fig. 6.

The first step in adjusting the 117-foot waveguide was to set all of the probes at the same angle and then adjust tie lines  $L_1$  and  $L_2$  to the

same electrical length. The tie lines were cut to the same physical length and joined through a tee-fitting. They then were adjusted in length until equal currents were obtained on the two center slots of the waveguide when power was supplied to the center connection of the tee-fitting. Following this operation, all of the slot probes on the south half of the guide were adjusted so as to obtain approximately the theoretical desired current distribution shown in Fig. 15. Each probe on the north half of the guide then was set to the same angle as the corresponding probe on the south half of the guide. The procedure was followed a second time and complete readings were made of slot currents. Figure 19 is an interior view of one end of the guide which shows the 25-inch excitation probe and two of the slot probes adjusted to give the desired current ratios at their respective slots. No attempt was made to establish an optimum length for the excitation probes.

Prior to matching, the VSWR observed at the sideband input of the r-f bridge was approximately 12 to 1, and the VSWR at the carrier input of the bridge was less than 3 to 1. A 90° change in length of the two tie lines,  $L_1$  and  $L_2$ , decreased the VSWR at the sideband input of the bridge to approximately 2.5 to 1, but resulted in a VSWR of 15 to 1 at the carrier input of the bridge. By adjusting the lengths of both of the tie lines and of the r-f bridge elements, it was possible to obtain a VSWR of approximately 2.5 to 1 at the carrier and sideband inputs of the bridge simultaneously.

The procedure followed in determining the lengths  $L_1$ ,  $L_2$ ,  $L_3$ ,  $L_4$ ,  $L_5$ , and  $L_6$  was to make  $L_3$ ,  $L_4$ , and  $L_5$  each one-quarter wavelength long and  $L_6$ , three-quarters wavelength long, select two equal random lengths for  $L_1$  and  $L_2$ , and then measure the VSWR at the carrier and the sideband inputs of the bridge. As  $L_1$  and  $L_2$  were maintained equal but were changed in small amounts simultaneously, the VSWR would be observed to change at the two input corners of the bridge. The object was to reduce the VSWR to a minimum at each input corner of the bridge using a given length of tie line. It was necessary to change the lengths of all four of the bridge legs before a length of the tie lines was found which permitted a low VSWR to exist in both the carrier and sideband inputs of the bridge before matching. The slot currents then were rechecked and the settings of the probes were readjusted slightly in accordance with the procedure outlined above. The r-f feed lines to the bridge then were matched to a VSWR of less than 1.1 to 1.

Field patterns were measured with the waveguide excited by unmodulated r-f energy supplied first to the sideband and then to the carrier inputs of the r-f bridge. The minor lobes were found to have an amplitude less than 10 per cent of the major lobes of the carrier and of the sideband patterns. When Fiberglas covers were placed over the slots, no measurable difference was noted in either the amplitude or the shape of the recorded field patterns. Tests for vertical polarization of the signal from the waveguide were made along course with a portable polariscope mounted in the plane and in the instrument truck. No polarization error was noted in either case.

### Field Strength Ratios and R-F Phasing.

A comparison of the carrier field strength of the waveguide and the carrier field strength of the clearance array, when each was fed the same amount of power, showed the waveguide to have a gain of approximately 9 db along the extended centerline of the runway. It was noted that the field strength of the clearance array was about 6 db lower in the direction of the runway than it was in the opposite direction. There was no change in the front-to-back ratio of the carrier field pattern after the spacing of the carrier loops was increased to 150° to obtain more clearance.

An earlier report<sup>6</sup> states that phase error due to proximity of the observer to an antenna array may be closely approximated by the formula

$$e = \frac{-A^2 \cos^2 \phi}{8D}$$

where the error  $e$  is expressed as the difference in length between the observer and the ends and the center of the antenna array,  $A$  is the total aperture of the array,  $D$  is the distance between the observer and the center of the array, and  $\phi$  is the azimuth of the observer with respect to the array, measured from the normal. It will be noted by inspection of the formula that the error in phasing varies inversely with the distance from the antenna array. This is shown in Fig. 20. When using the above formula for calculating the two curves in Fig. 20, an equispaced, three-element, linear array with an aperture of 102 feet was assumed.

Proper phase relationship between the carrier and the sideband inputs to the r-f bridge feeding the waveguide was determined by the quadrature method. An instrument truck equipped with a Collins 51R3 receiver was located at a point 5,000 feet from the station and 2 1/2° off the runway centerline. At this point, due to proximity between the ends and the middle of the waveguide array, the phase error was considered to be approximately 5°. A 90° length of r-f line was inserted in the carrier feed line and the r-f phaser was adjusted until the CDI current in the instrument truck was reduced to zero, indicating quadrature relationship between the carrier and the sideband. The added 90° length of r-f line in the carrier feed line then was removed and the attenuator in the hybrid unit of the associated sideband generator rack was adjusted until the CDI read full scale.

A similar procedure was followed in the adjustment of the clearance array. Because the field strength of the clearance array is much lower than the field strength of the waveguide array, the clearance array does not control the receiver within 5° of the course established by the waveguide. Considerable latitude exists in the setting of the attenuator pad in the

<sup>6</sup>Chester B. Watts, Jr., op. cit.

<sup>7</sup>Watts, Taggart, and Voyles, op. cit.

hybrid unit used with the sideband generator which supplies power to the clearance array. It is therefore possible to obtain almost any width desired for the rear course independently of the front course.

A change in the ratio of the field strengths of the two arrays can be accomplished by changing the power delivered to the clearance array. The optimum ratio depends upon the magnitude of the minor lobes of the waveguide array and on the desired distance range of the installation at right angles to the course. If the ratio is set too low, the waveguide will lose control of the receiver and the effectiveness of the waveguide in suppressing bends or scalloping will be reduced. If the ratio is set high, the distance range of the system perpendicular to the course will be reduced or there may be points of low clearance at certain bearings from the station.

In order to determine the optimum field strength ratio, recordings of CDI current were made at an altitude 1,000 feet above ground while flying a semicircle of 6 miles' radius across the front course. A Collins 51R3 receiver was employed. Recordings in Figs. 21A, 21B, 21C, and 21D show the effect of using different ratios of field strength on clearance.

Figure 21A shows the CDI current recorded when the ratio of the field strength of the carrier of the waveguide to the carrier of the clearance array is 3.35. The course width is approximately  $4.8^\circ$  and the crossover is smooth. There are no points of low clearance.

Figure 21B is a recording of CDI current when the ratio of field strength of the carriers of the two arrays is 4.41. It will be noted that there is a small decrease in clearance on each side of the course beyond full-scale reading of the CDI.

Figure 21C shows the effect of further increasing the ratio of the carriers of the two arrays to 6.06. At  $18^\circ$  the CDI current is 168 microamperes, whereas at the corresponding point in Fig. 21B, the CDI current is in excess of 214 microamperes. This demonstrates the effect of the minor lobes of the waveguide on the clearance of the system. This is the adjustment considered optimum consistent with operating requirements.

In Fig. 21D, the power to the clearance array was reduced to the lowest value tested. The ratio of the field strength of the two carriers was 8.08. While the crossover remained smooth, the clearance decreased to a value of 142 microamperes at  $18^\circ$  azimuth, which is below the full-scale value of 150 microamperes.

Figures 22A, 22B, and 22C are recordings obtained on orbital flights at a distance of 6 miles from the directional localizer. They were made while the field strength ratio of the carriers of the two arrays was 6.06.

Figure 22A is a recording of the CDI current made while circling the station with sideband and carrier power supplied only to the waveguide. The recording while flying across the course is smooth. Maximum clearance is obtained at approximately  $4^\circ$  on each side of the course. It will be noted that the clearance, when the waveguide is operated alone, decreases beyond  $4^\circ$  until it becomes zero at approximately  $10^\circ$  on each side of the "on course" position. These are the points at which the effect of the clearance array is greatest because the space modulation of the clearance array is greatest. It is in the sector between these points where capture effect<sup>8</sup> permits the waveguide to exercise greatest control over the operation of the receiver.

Figure 22B, a recording of CDI current with only the clearance array in operation, shows the low-clearance points at  $22^\circ$  on each side of the front and rear courses which is typical of 8-loop localizers. It will be observed that the width of the front course is approximately  $5^\circ$ , whereas the width of the rear course is slightly less than  $4^\circ$ . This difference in course width is believed to be due to the presence of the waveguide.

Figure 22C is a recording of the CDI current made with both the clearance array and the waveguide array in operation. At  $8^\circ$  on each side of the front course, there are slight decreases in the amount of clearance. As the clearance array assumes more control of the receiver and as the space modulation of the clearance array carrier by the clearance array sidebands increases, reaching a maximum at  $10^\circ$ , the CDI current increases to more than 250 microamperes. In this recording, the CDI current remains above 250 microamperes except at a point about  $20^\circ$  on each side of the front and rear courses, where low clearance ordinarily is encountered from an 8-loop localizer.

Figure 23A is a recording of CDI current during a low approach from a point 10 miles from the station when only the clearance array was in operation. The airplane was aligned with the runway visually by the pilot during this flight. Deviations of 25 microamperes to the left and 18 microamperes to the right will be noted in the CDI current and many smaller variations can be seen.

Figure 23B is a recording of CDI current variation when the waveguide only was in operation, but with other conditions the same as in Fig. 23A. In this case, the CDI deflection is 11 microamperes left and zero. The random excursions in CDI current are less than those in Fig. 23A.

Figure 23C shows the CDI current variation during a low approach when both the clearance array and the waveguide were in operation. Maximum departure from "on course" indication was 12 microamperes left and zero. The random variations are of similar frequency and magnitude as in Fig. 23B,

<sup>8</sup>Chester B. Watts, Jr., op. cit.; Watts, Taggart, and Voyles, op. cit.

indicating that the waveguide was controlling the receiver when both arrays of the directional localizer were in operation.

### SITING TESTS

Ground and flight tests were conducted to investigate the comparative effect of a nearby reflecting object on the courses of the conventional and the directional localizer. A vertical screen comprising the reflecting object was positioned first in front of, and later behind, the antenna system. Portable towers supported the vertical screen which consisted of eight horizontal aluminum wires, one above the other, spaced 8 inches apart and 100 feet long. The wire screen could be raised to a height of 55 feet above ground level. Figure 24 is a view of the vertical screen reflector positioned in front of the antenna system. As shown, it is 450 feet in front of the clearance array and approximately  $23^\circ$  from the course line. An instrument truck equipped with an aircraft-type "ram's horn" receiving antenna, a Collins Type 51R3 receiver, and necessary recording equipment were used in these tests. The truck was driven on the runway centerline from approximately 2,300 feet to a point within 800 feet of the localizer antennas. Checks also were made crossing the course 900 feet from the localizer antennas. Recordings were made with the reflector positioned at various distances from the course line ( $\theta = 2.8^\circ$  to  $25.2^\circ$ , Fig. 25) for the conventional localizer, the directional localizer, and the slotted waveguide. The tests were made with the axis of the vertical screen reflector parallel and also perpendicular to the localizer courses.

"Siting error" is defined as the difference between the number of degrees traversed by the course deviation indicator (extremes plus to minus) with the test screen in place and with the test screen removed.<sup>9</sup> This error in a localizer results from unequal 90- and 150-cps signal components in a receiver which is located on the localizer course. The inequality between the 90- and 150-cps signals is a function of the r-f phase difference between the direct and reflected signals. The curve in Fig. 25 illustrates, for one siting condition, the rate of change in r-f phase difference between the direct and reflected signals as the receiver moves along the localizer course. Referring to the diagram in Fig. 25, the difference in distance  $\psi$  traveled by the direct and reflected signals arriving at a receiver ( $x + b$ ) distance from an antenna can be expressed by:

$$\begin{aligned}\psi &= x + b - (a + d) \\ &= x + b - \frac{b}{\cos \theta} - \sqrt{b^2 \tan^2 \theta + x^2}\end{aligned}$$

<sup>9</sup>S. R. Anderson and H. F. Keary, "VHF Omirange Wave Reflections from Wires," Technical Development Report No. 126, May 1952, pp. 1 and 9, Fig. 15A.

$$\begin{aligned}
 &= x + b - \frac{b}{\cos \theta} - b \sqrt{\tan^2 \theta + \left(\frac{x}{b}\right)^2} \\
 &= x + b \left( 1 - \frac{b}{\cos \theta} - \sqrt{\tan^2 \theta + \left(\frac{x}{b}\right)^2} \right) \quad (1)
 \end{aligned}$$

where

$\psi$  = difference in distance in feet traveled by the direct and the reflected signal arriving at a receiver.

$a$  = distance in feet from clearance array to center of vertical screen reflector.

$\theta$  = bearing of center of vertical screen reflector from clearance array with respect to centerline of runway.

$b$  =  $a \cos \theta$ .

$d$  = distance in feet from receiver to center of vertical screen reflector.

$\phi$  = bearing center of vertical screen reflector from receiver with respect to centerline of runway.

$x$  =  $d \cos \theta$ .

By differentiating equation (1), an expression for the rate of change in with respect to distance  $x$  becomes

$$\frac{d\psi}{dx} = 1 - \frac{1}{\sqrt{1 + \frac{b^2}{x^2} \tan^2 \theta}} \quad (2)$$

A change in  $\psi$  equal to one wavelength causes one cycle of scalloping on the localizer course. Also, when  $\psi$  is expressed in wavelengths, the term  $\frac{d\psi}{dx}$

becomes wavelengths divided by feet. In view of these relationships, values for the quantity  $\frac{d\psi}{dx}$  were obtained from test recordings by dividing portions

of scalloping cycles by the distance in which they occurred. Figure 25 shows a plot of equation (2). The measured values, indicated by the circled points, are for one set of conditions used in the siting tests. These are in close agreement with the theoretical curve. The curves in Fig. 26 show other measured values of  $\frac{d\psi}{dx}$  with the reflector at various off-course positions.

The field intensity of the reflected wave may be used to predict the relative amplitude of siting error which will be produced by a vertical

sheet reflector. Two factors that determine the field intensity of the reflected wave are the projected reflector area normal to the arriving signal and the relative field strength of the localizer sidebands. From the diagram in Fig. 27, it will be noted that the projected reflector area normal to the arriving wave can be represented by  $\sin \alpha$ . The relative field strength of the localizer sideband accounts for all departures of the course deviation indicator from center. Relative siting error  $S$  caused by a vertical sheet reflector representative of the conditions of one series of tests performed then is expressed by

$$S = kf(\theta) \sin \alpha \quad (3)$$

where

$k$  = a constant depending upon such factors as the reflection efficiency of the screen reflector,

$f(\theta)$  = the relative field strength of the localizer sideband at the "off-course" angle  $\alpha$ ,

$\alpha = \theta$  from the geometry as shown in the diagram of Fig. 27.

The curves in Fig. 27 illustrate the theoretical siting error of the conventional and directional localizers which will be produced by a horizontal wire or vertical sheet reflector positioned parallel to the localizer course. The circled points represent measured values of siting error for a conventional localizer and the triangular points represent measured values of siting error for the directional localizer.

"Bend reduction factor" is defined here as the ratio of the absolute value of directional localizer siting error to the absolute value of conventional localizer siting error, where the siting error in each case is produced by the reflector.<sup>10</sup> The theoretical bend reduction factor is shown in Fig. 28. The circled points represent measured values obtained during these tests.

Another series of tests was conducted with the vertical screen oriented perpendicular to the localizer course. Individual recordings were made for several values of  $\theta$ , where  $\theta$  represents the angle formed by an extended runway centerline and a line from the center of the antenna array through a point at the end of the screen nearest the course. See Fig. 29. Figure 29 shows the measured rate of change of  $\psi$  with respect to distance  $x$  for several positions of the vertical screen. The scalloping frequency for the directional localizer when  $\theta$  was equal to  $5.6^\circ$  was very low, causing  $\psi$  to remain almost constant. Figure 30 shows the measured siting errors with the screen positioned perpendicular to the localizer course.

<sup>10</sup>Chester B. Watts, Jr., op. cit.



Figures 31 and 32 are flight recordings of CDI current made when the vertical screen reflector was positioned in front of the antenna system. The reflector was placed parallel to the course with the midpoint approximately  $23^\circ$  off course. Figures 31A and 32A are recordings for the clearance localizer operating only, and Figs. 31B and 32B are recordings for the directional localizer.

It will be noted that CDI excursions of approximately 2.66 dots ( $80 \mu a$ ) exist on the low approach recording shown in Fig. 31A, but are not present in Fig. 31B when the directional localizer is in operation. Figure 32A is a recording of the CDI oscillations caused by the reflector while flying across the course at a distance of 15 miles with the clearance localizer in operation. In Fig. 32B, the CDI oscillations are absent and the recording shows a smooth crossover as a result of the operation of the directional localizer.

Figures 33 and 34 are CDI current recordings made when the vertical screen reflector was in back of the antenna system as shown in Fig. 35. Figure 33A represents a low approach with only the clearance localizer in operation, and Fig. 33B is a recording of a low approach with the directional localizer in operation. Figure 34A is a recording showing CDI oscillations while flying across the course 15 miles from the station with the clearance localizer in operation, and Fig. 34B is a similar test with the directional localizer in operation. These recordings illustrate conclusively the effectiveness of the directional localizer in producing a straight course.

#### OPERATIONAL TESTS

The directional localizer using the 117-foot waveguide was tested over a period of 5 weeks. During this time, the transmitting equipment was operated continuously and no tuning adjustments or changes of any kind were made. When measurements of course width or course position of either the waveguide or the clearance arrays were made, plate voltage was removed temporarily from the transmitting equipment supplying the array which was not being tested. An instrument truck on which a Yagi receiving antenna was mounted was driven to a point near the far end of the runway served by the localizer where careful checks of course width and course position were made. Readings were taken in midmorning or late afternoon after the receiving equipment had been permitted to warm up for 1 hour. Occasionally, readings were taken in both the morning and the afternoon. Carrier and sideband power supplied to each array was read with a "Feed-Thru" wattmeter.

Figure 36 is a bar graph showing the variation in course width during the 5-week period that the localizer was operated continuously. The height of each bar indicates the amount of error in course width from the normal width of  $5^\circ$ . The total deviation of the waveguide array operating by itself was  $0.9^\circ$ , whereas the total deviation of the clearance array operating alone was  $2.1^\circ$ . When both arrays were supplied with power simultaneously, the total deviation in course width was  $0.7^\circ$ . The similarity of the graphs of course width measured when the waveguide was operating by itself, and when both the

waveguide and the clearance array were in operation, indicates that the waveguide controlled the course width of the localizer when both arrays were operating. During the 5-week test period, the output of each sideband generator decreased nearly 20 per cent. Course deviation, as shown in Fig. 36, was obtained by modifying the measured values of course width to take into account the effect of changing output of the sideband generators. No other corrective factors were applied to the recorded data.

Figure 37 is a bar graph which shows the variation of course position during the 5-week test period. Maximum course position deviation of the waveguide was  $0.144^\circ$ , whereas the maximum course position deviation of the clearance array was  $0.2^\circ$ . When the two arrays were in operation, the maximum course position deviation was  $0.133^\circ$ . The similarity of the deviation measured when the waveguide was operating by itself, and when it was operating in conjunction with the clearance array, is additional evidence that the course of the directional localizer is controlled by the waveguide.

### CONCLUSIONS

The following desirable features of a waveguide-type directional localizer were demonstrated:

1. The feed system of the waveguide has been simplified to the extent that only two r-f probes are required to excite the waveguide.
2. The course of the waveguide array is much more stable than the course of the eight-loop clearance array. This is true of both the course width and the course position.
3. Reflecting objects to the rear of the waveguide which cause the clearance array to be completely useless along course produce no measurable deviation in the course when the guide is placed in operation. Reflecting objects in front of the guide, and more than  $3^\circ$  to either side of the course, have only negligible effect on the course of the directional localizer. The effect of a reflecting object on the front course of the facility diminishes rapidly as its bearing from the localizer is increased.
4. Measurements of polarization error made along the front course of the facility while both the clearance array and the waveguide array were in operation showed that no polarization error was present. The measurements were made on the ground and in an airplane with a portable polariscope.
5. The waveguide is easy to construct. No unusual skills are required and, in general, ordinary techniques widely used in fabricating large air ducts are employed. It can be built by local contractors wherever it is installed.

In addition to demonstrating the above features of the waveguide-type directional localizer, it also was determined that the pattern sharpness of the 117-foot waveguide, operating as a clipped binomial array, is approximately the same as an array of 450-foot aperture operating as a full binomial array. Used in this fashion in conjunction with an eight-loop clearance array, it provides a front course which is essentially free of bends. The width of either the front or the rear course may be adjusted independently of the other. Clearance is adequate in all directions. The directional localizer is equally effective with either mechanical or electronic modulation.



FIG 1 FRONT VIEW OF 200-FOOT WAVEGUIDE

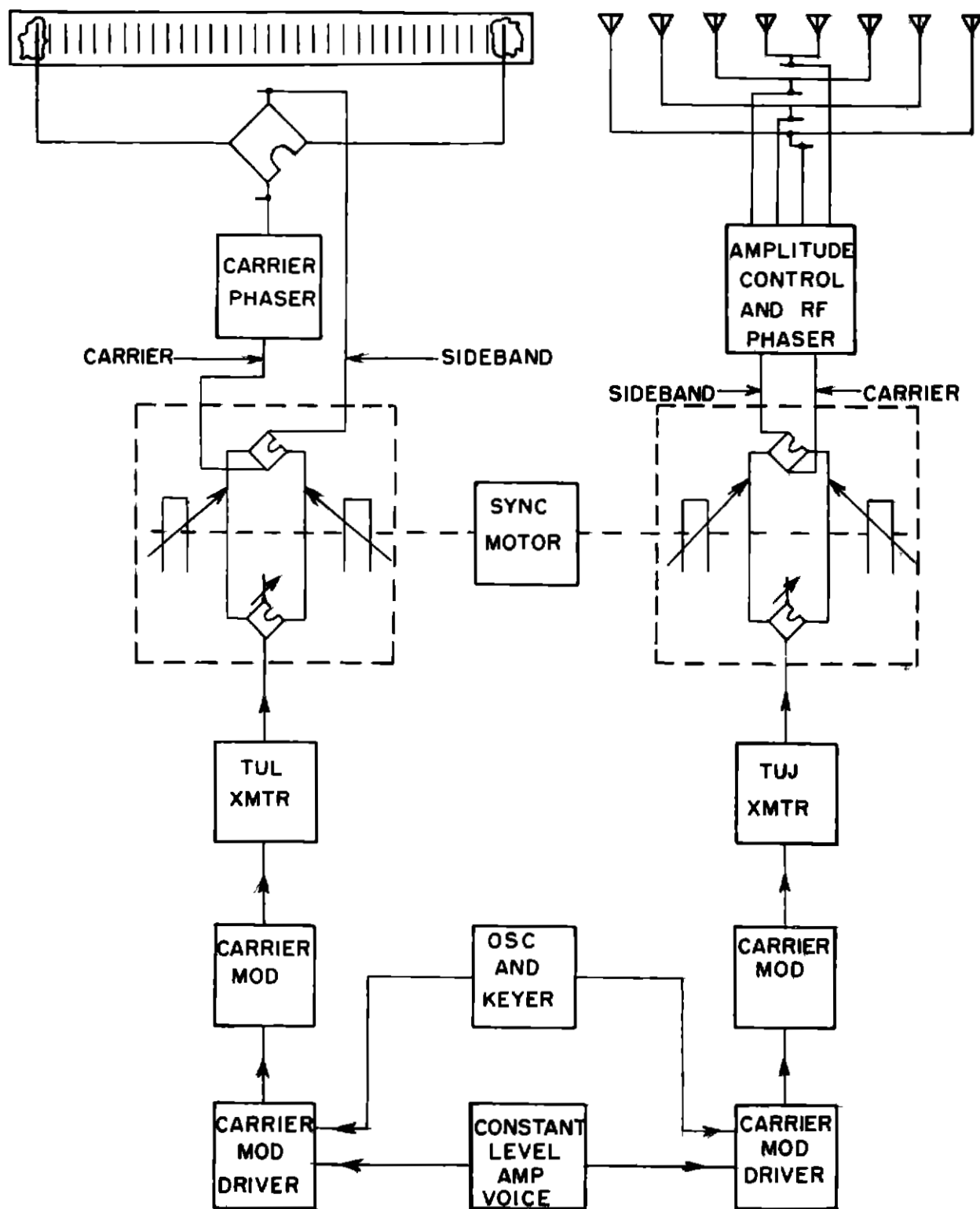
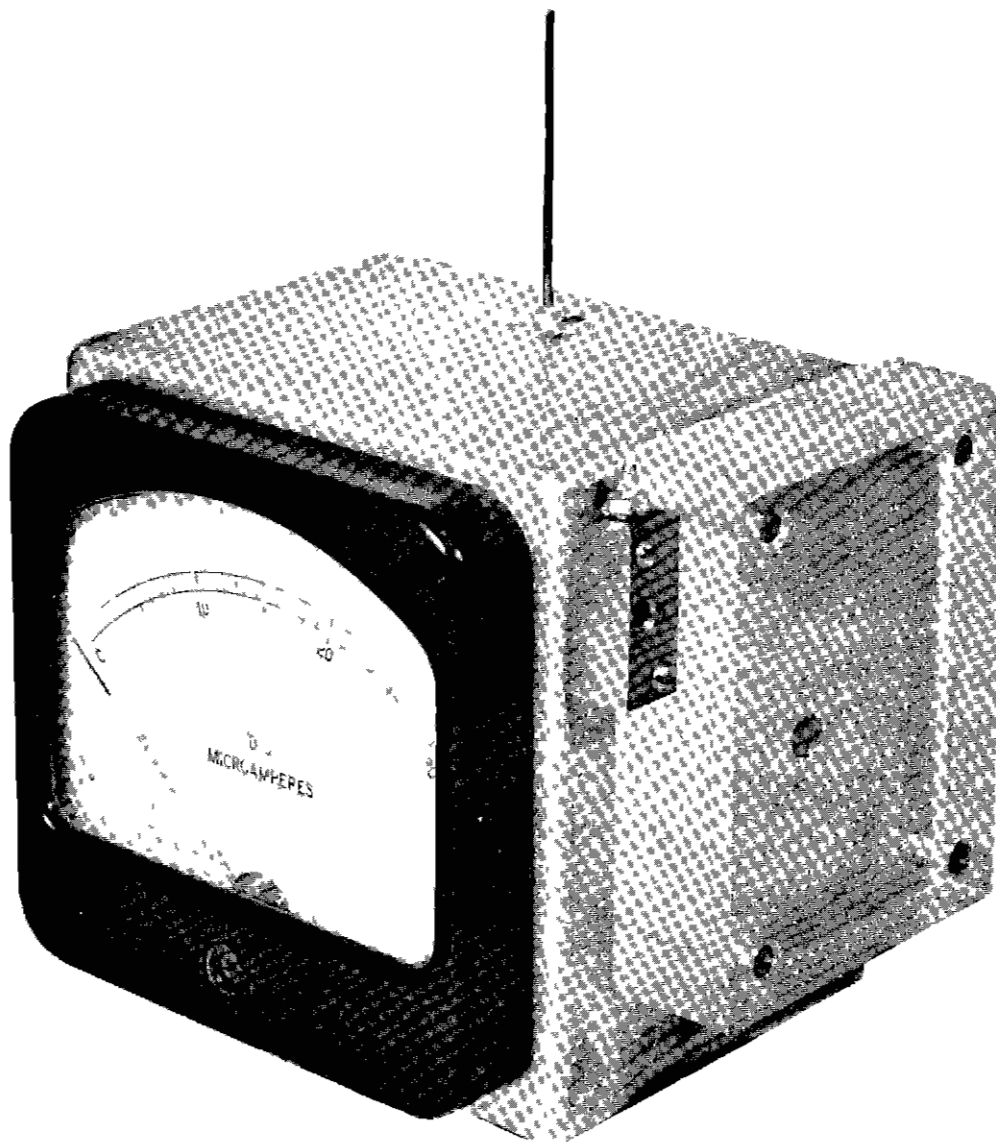


FIG 2 BLOCK DIAGRAM OF MECHANICALLY MODULATED DIRECTIONAL LOCALIZER WITH 200-FOOT WAVEGUIDE



CRA TECHNICAL  
DEVELOPMENT CENTER  
1501 N. W. 15th AVENUE

FIG 3 R-F MEASURING DEVICE - EARLY DESIGN

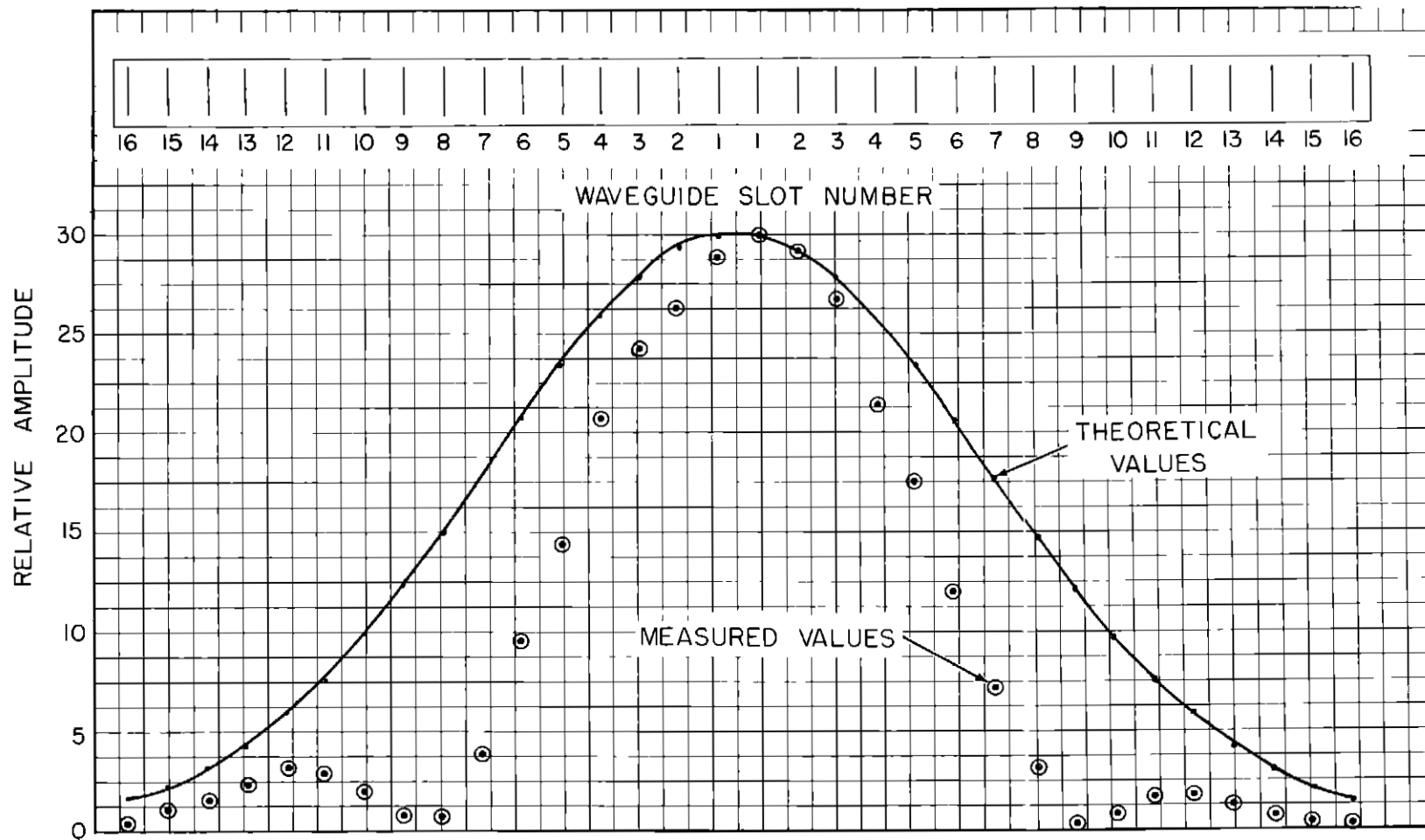


FIG 4 THEORETICAL AND MEASURED SLOT CURRENTS - CARRIER ONLY  
200-FOOT WAVEGUIDE

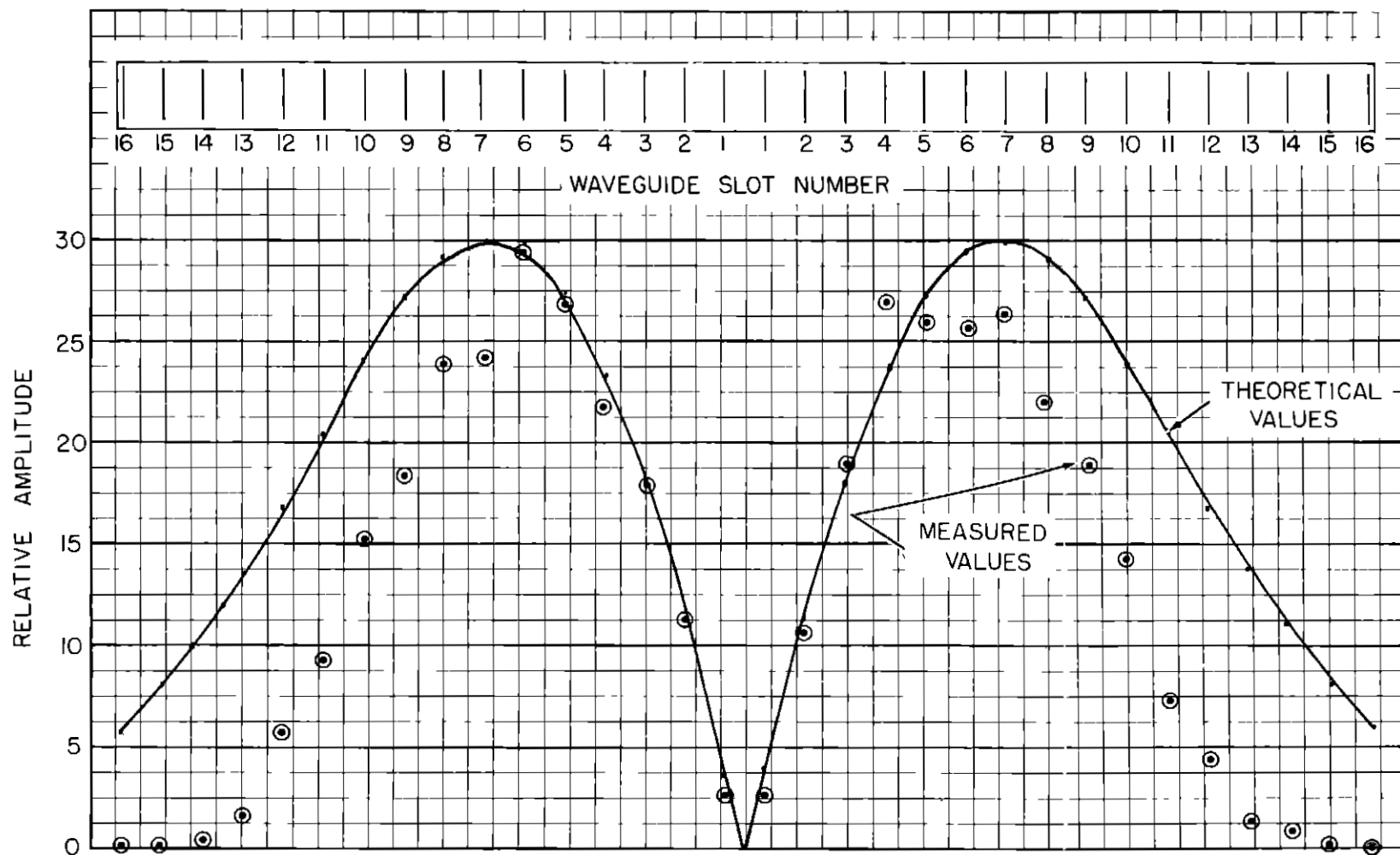


FIG 5 THEORETICAL AND MEASURED SLOT CURRENTS - SIDEBAND ONLY  
200-FOOT WAVEGUIDE



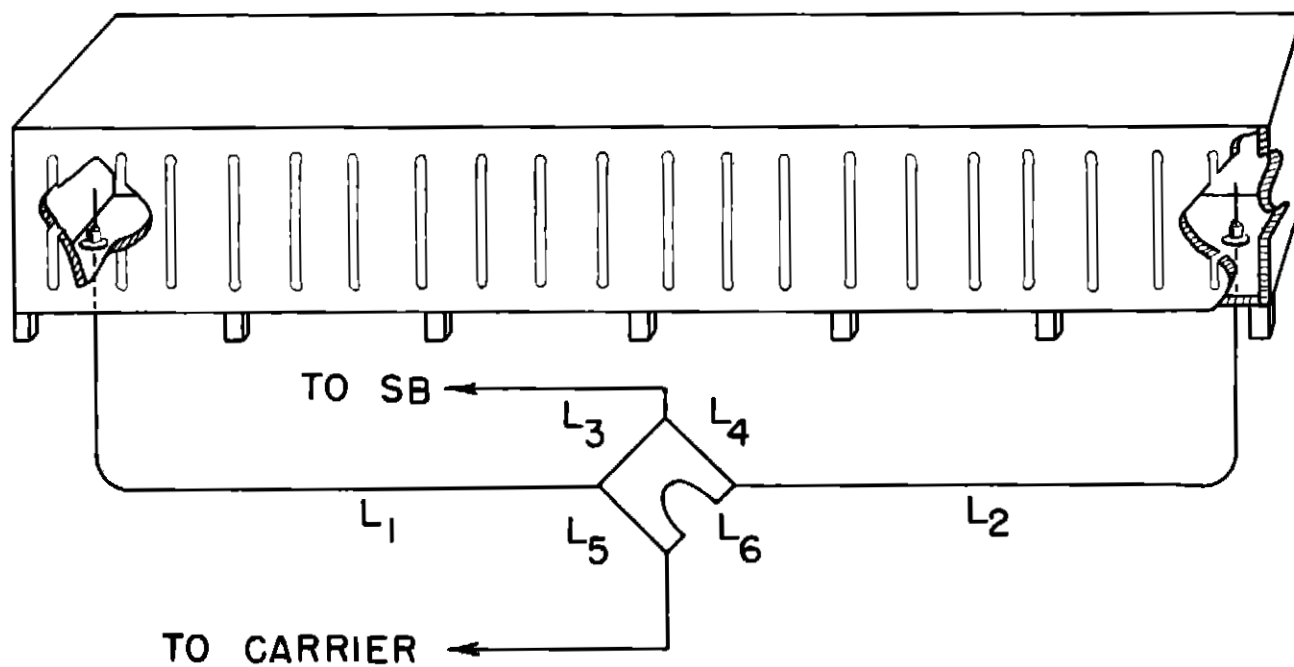


FIG 6 200-FOOT SLOTTED WAVEGUIDE - BRIDGE AND TIE-LINE ARRANGEMENT

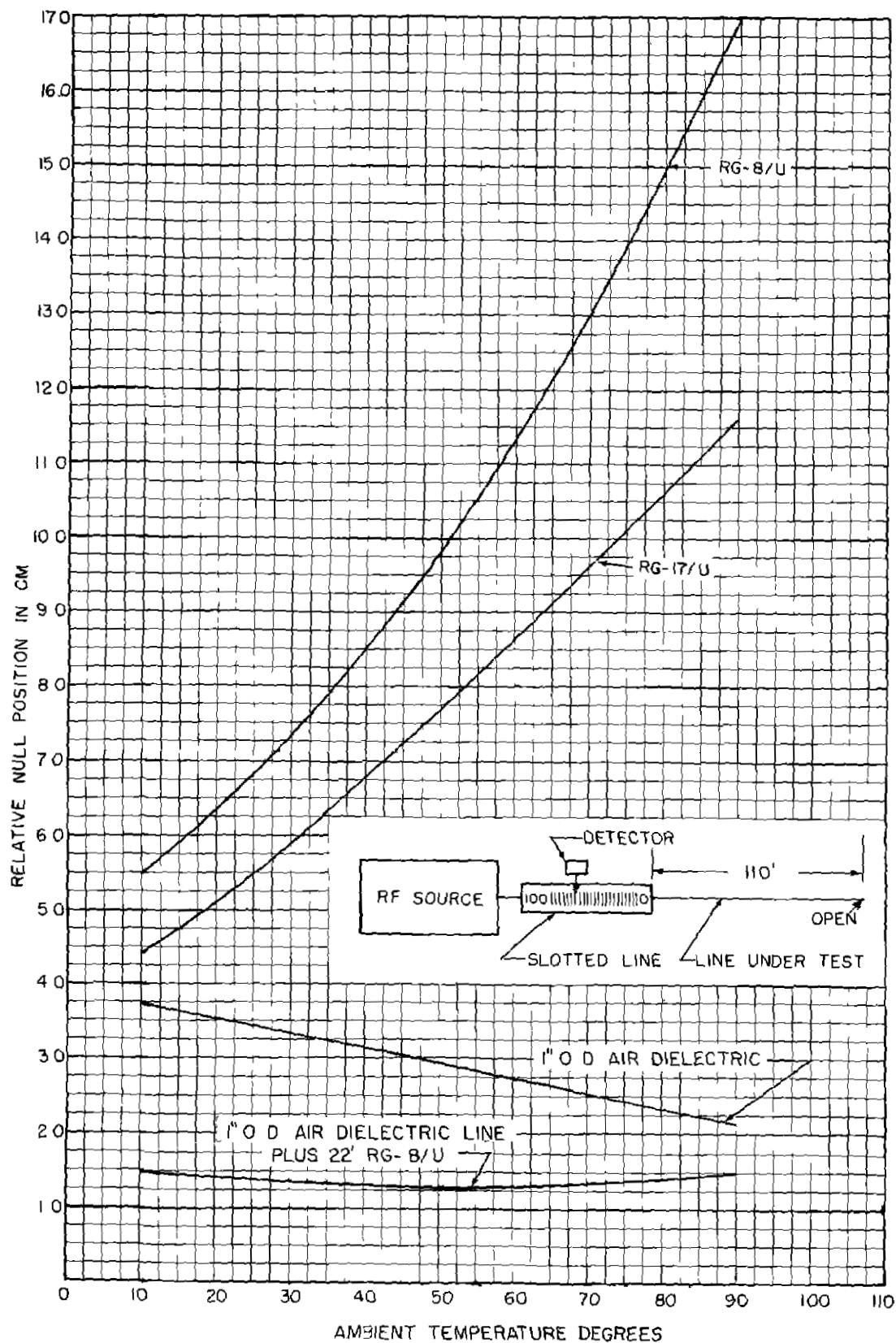


FIG 7 VARIATION IN ELECTRICAL LENGTH OF 110-FOOT LENGTHS OF R-F TRANSMISSION LINE WITH CHANGE OF AMBIENT TEMPERATURE

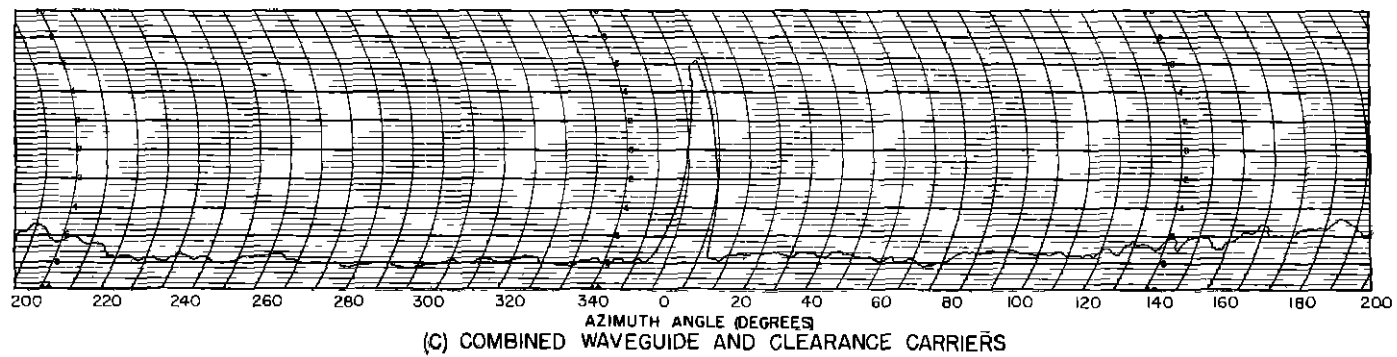
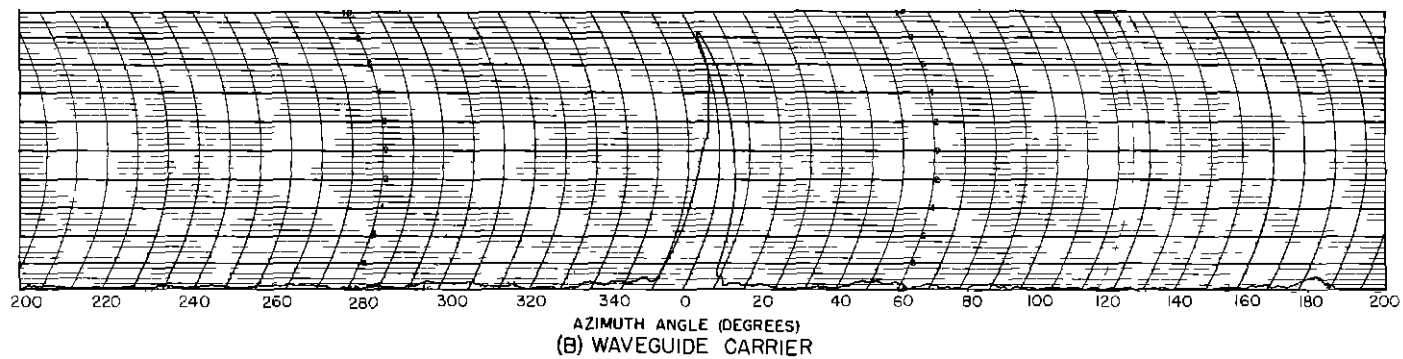
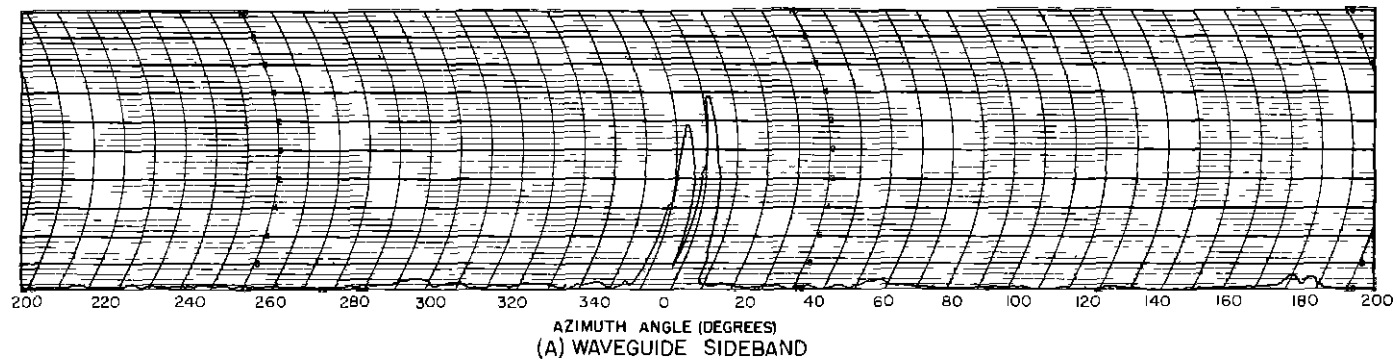


FIG 8 200 FOOT WAVEGUIDE ARRAY FIELD STRENGTH RECORDINGS

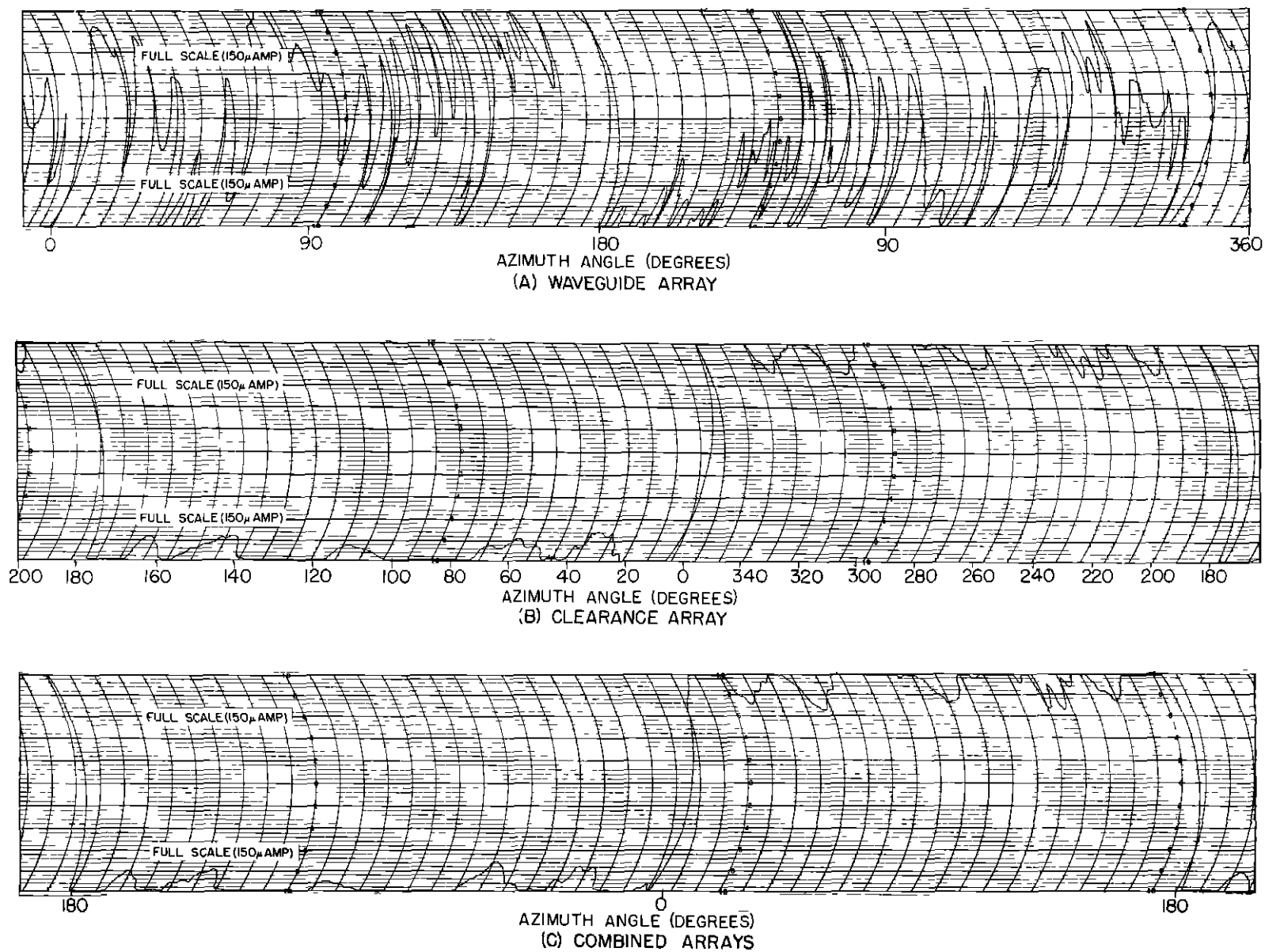


FIG 9 DIRECTIONAL LOCALIZER CDI CURRENT RECORDINGS USING 200-FOOT WAVEGUIDE ARRAY

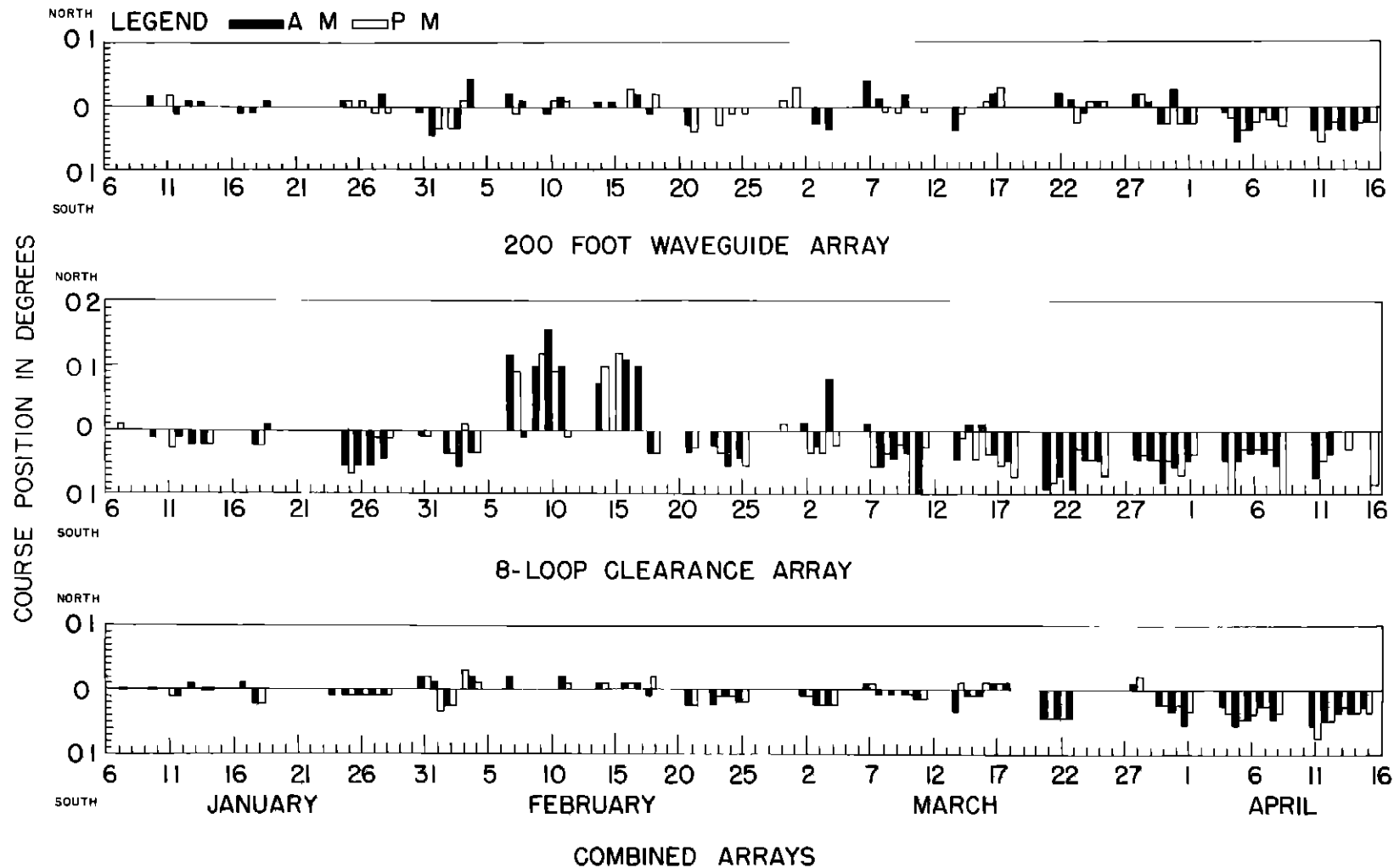


FIG 10 COURSE POSITION VARIATION OF DIRECTIONAL LOCALIZER  
USING 200-FOOT SLOTTED WAVEGUIDE

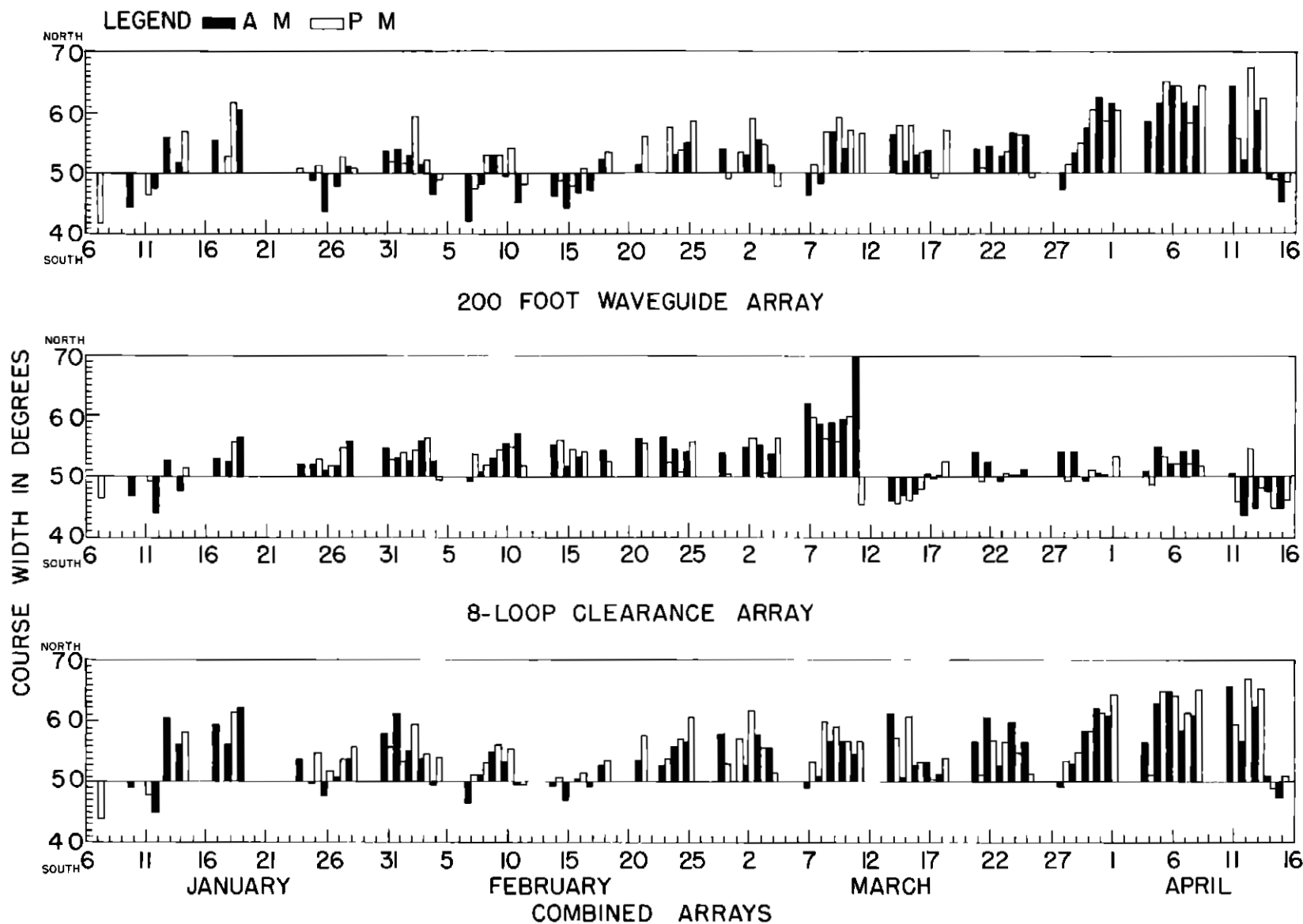


FIG 11 COURSE WIDTH VARIATION OF DIRECTIONAL LOCALIZER  
USING 200-FOOT SLOTTED WAVEGUIDE

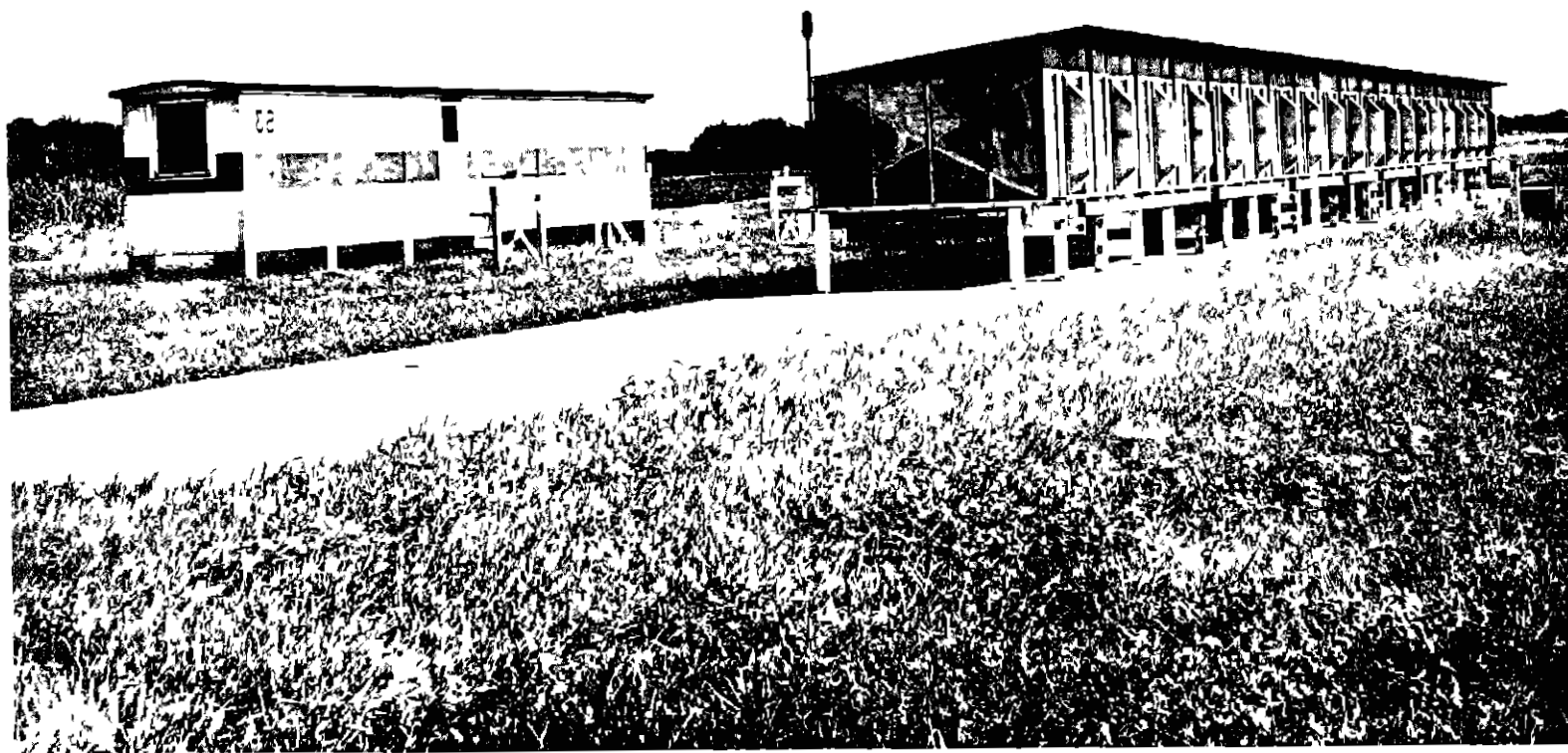


FIG 12 117-FOOT WAVEGUIDE AND 8-LOOP CLEARANCE ARRAY

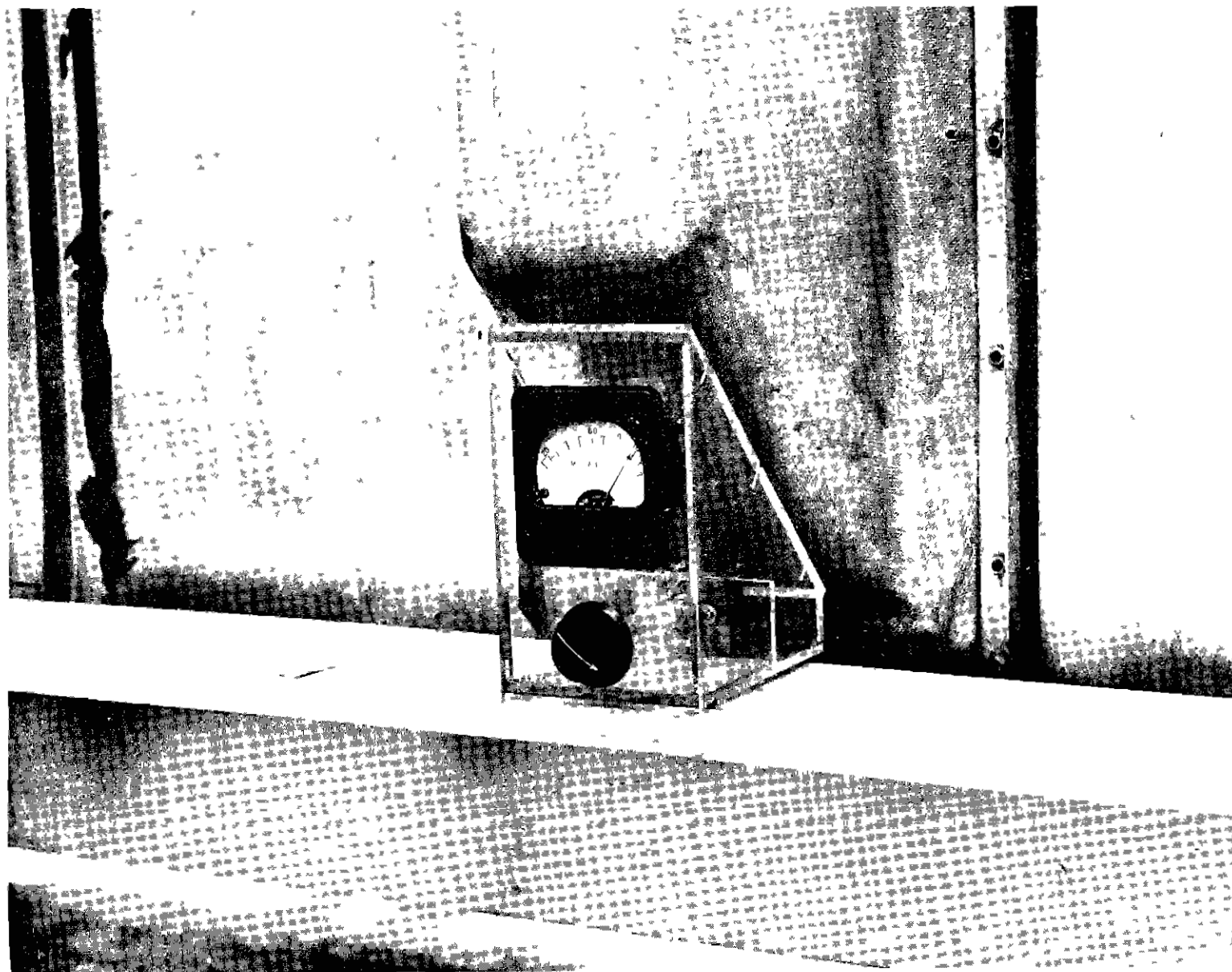


FIG 13 IMPROVED SLOT CURRENT INDICATOR



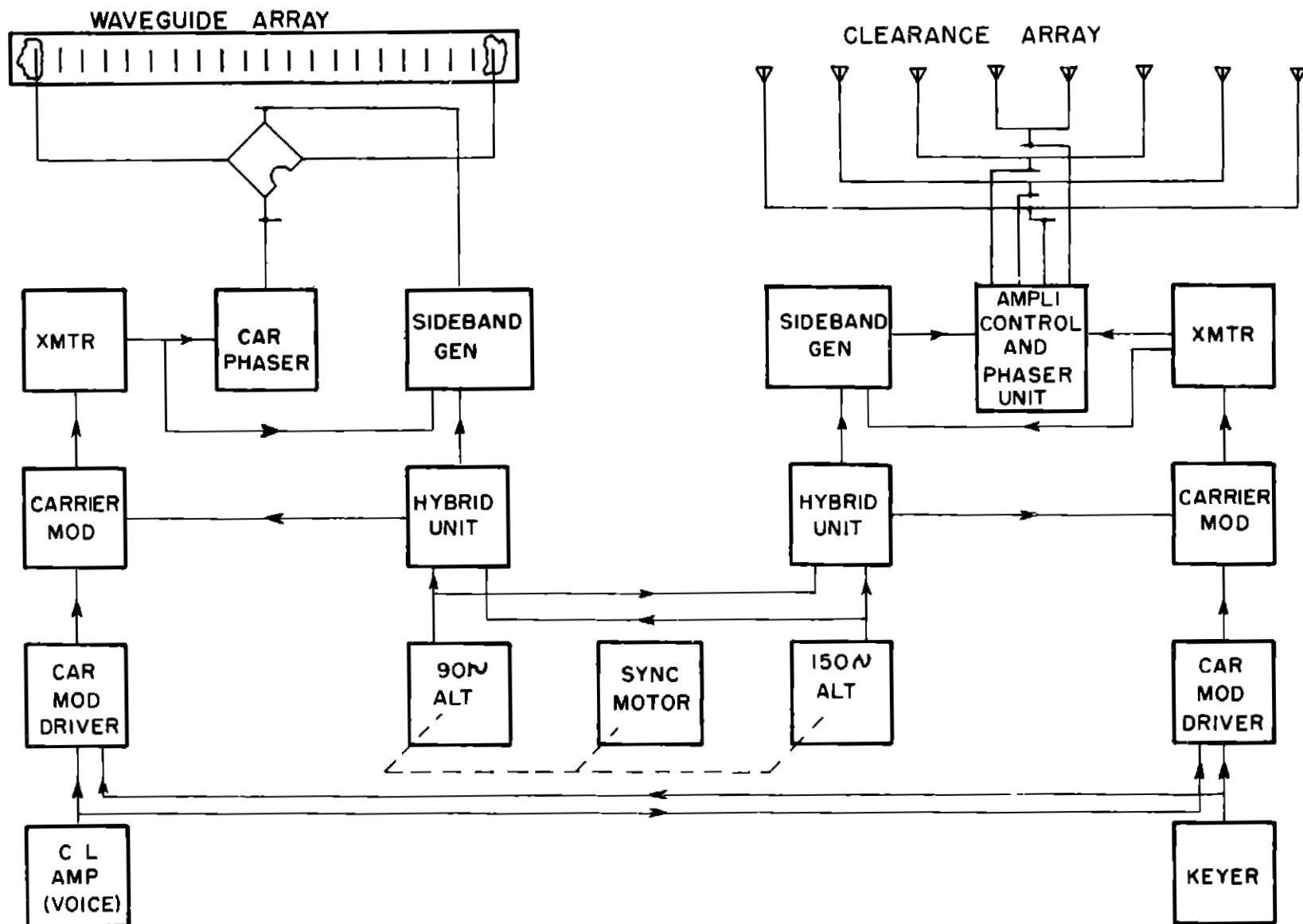


FIG 14 BLOCK DIAGRAM OF ELECTRONICALLY MODULATED DIRECTIONAL LOCALIZER WITH 117-FOOT WAVEGUIDE

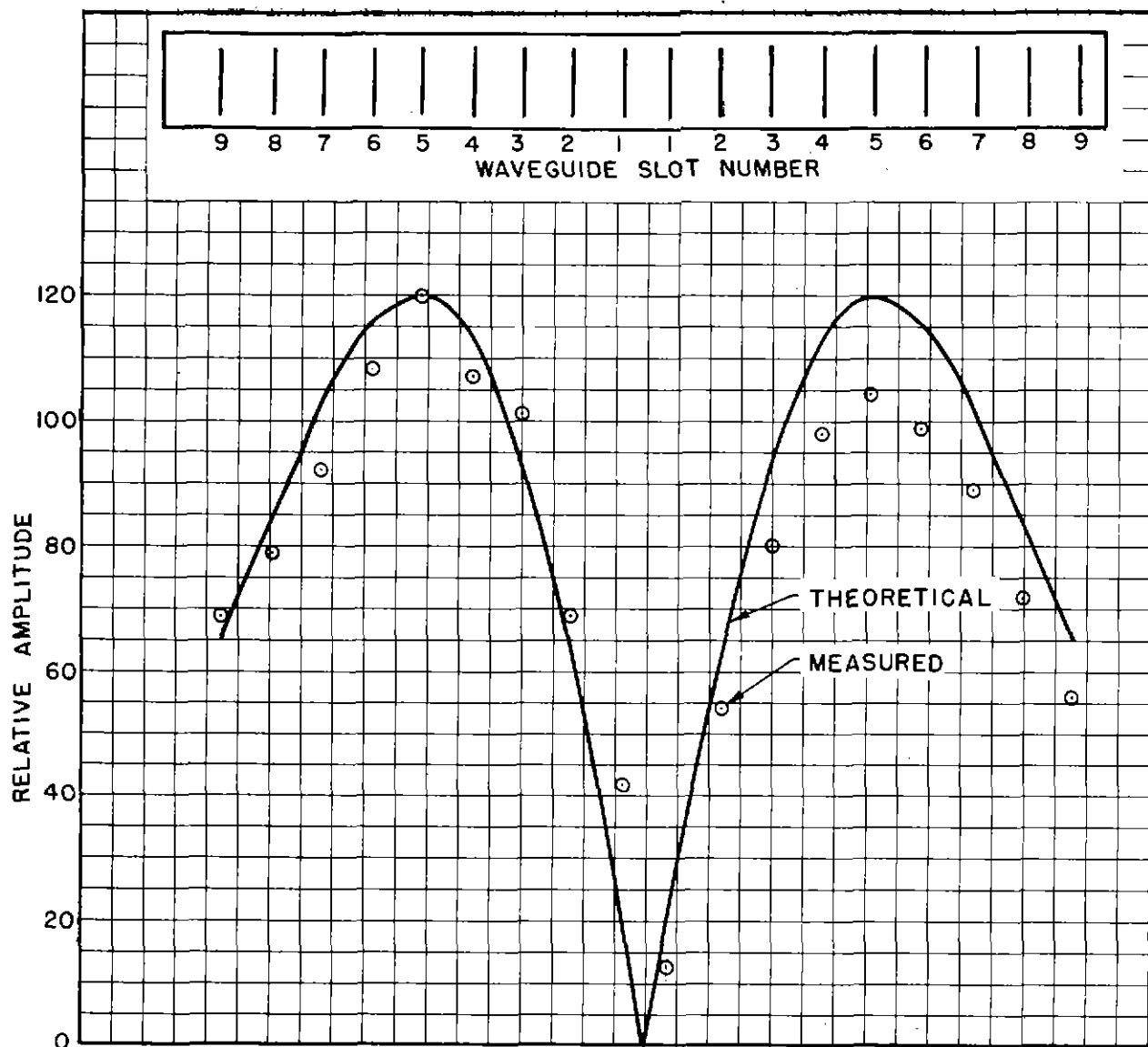


FIG. 15 THEORETICAL AND MEASURED SLOT CURRENTS - SIDEBAND ONLY  
117-FOOT WAVEGUIDE

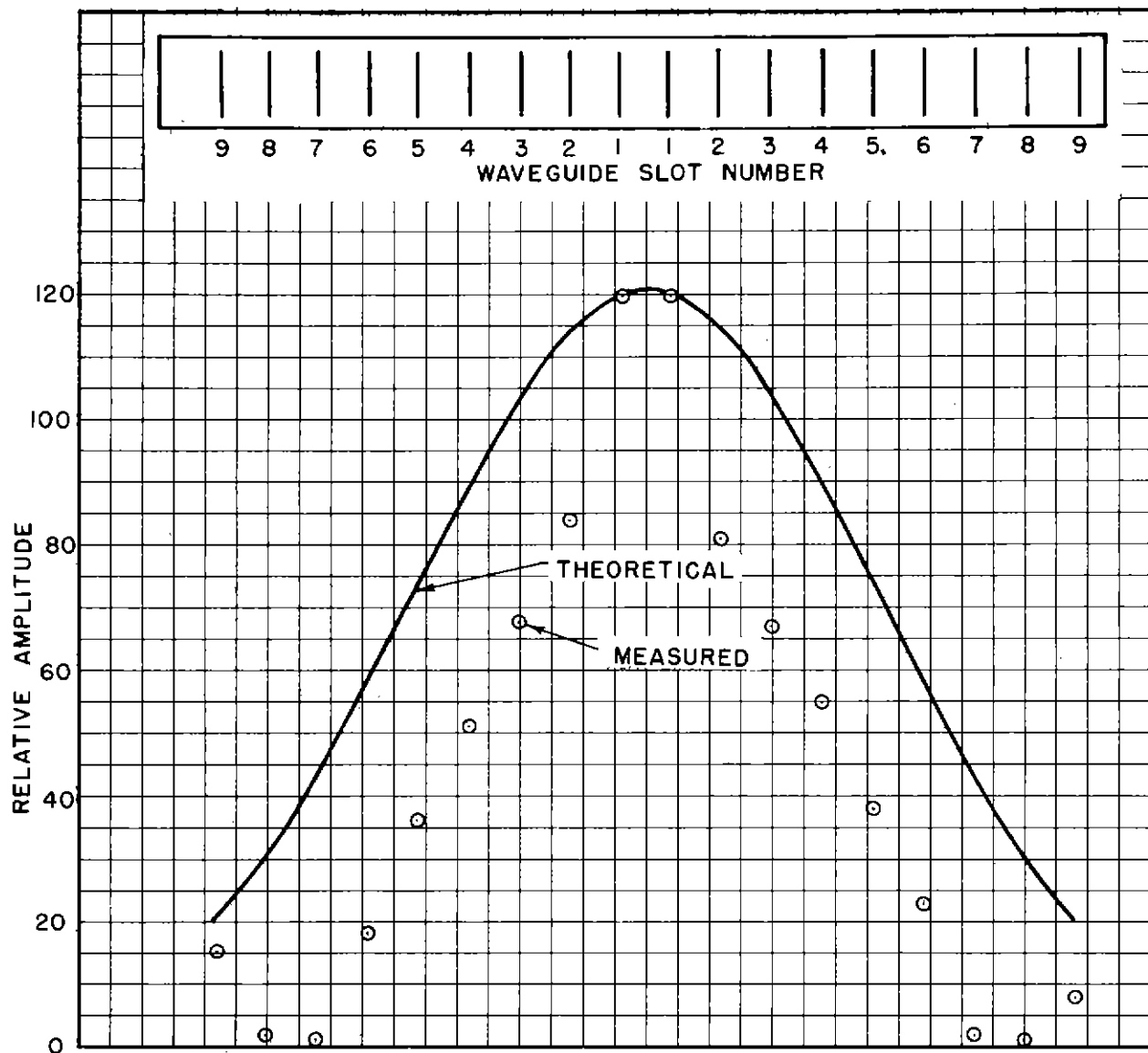


FIG. 16 THEORETICAL AND MEASURED SLOT CURRENTS - CARRIER ONLY  
117-FOOT WAVEGUIDE

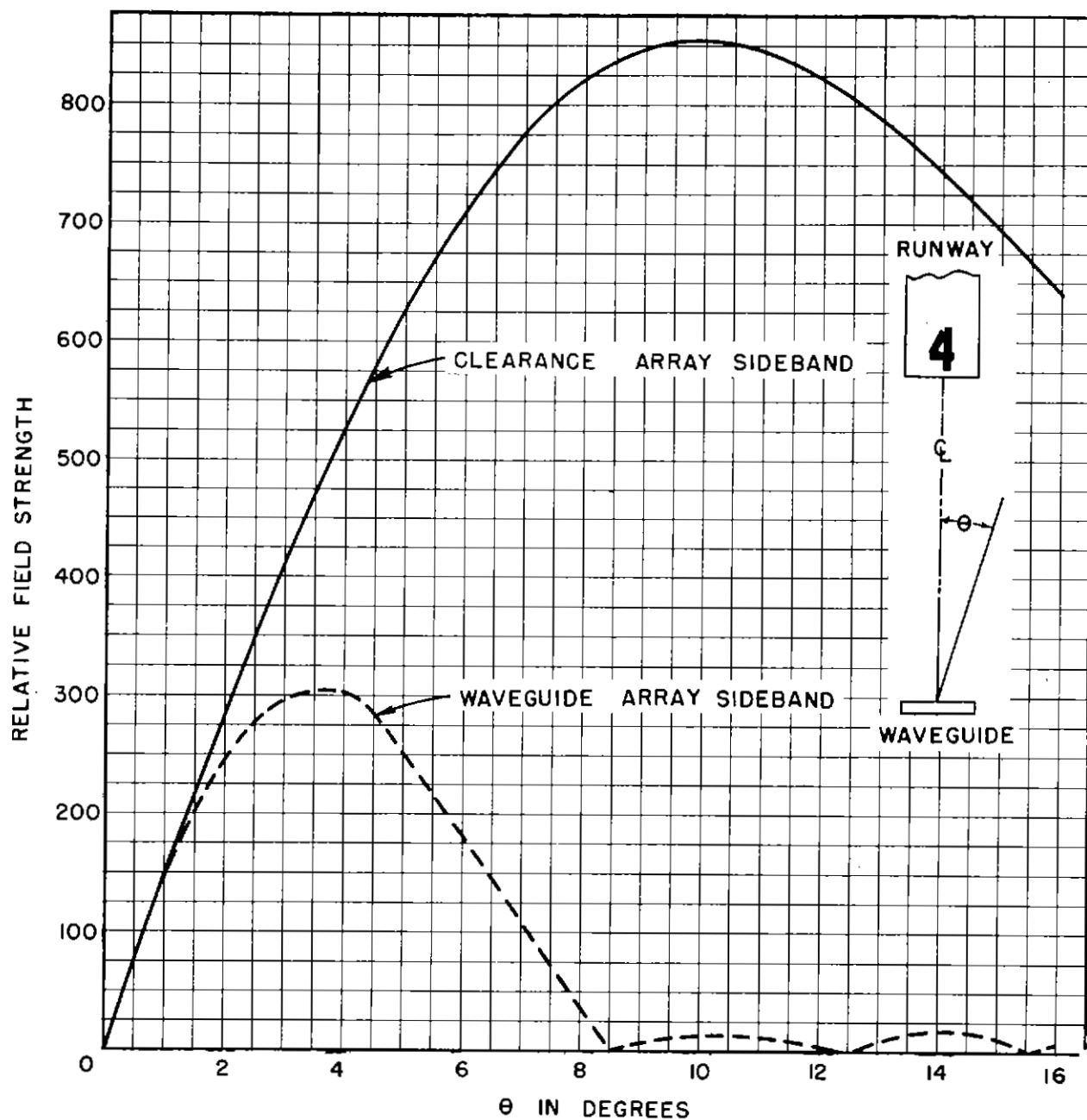


FIG. 17. RELATIVE AMPLITUDES OF WAVEGUIDE AND CLEARANCE SIDEBAND PATTERNS WHEN SET TO SAME SLOPE AT  $0^\circ$

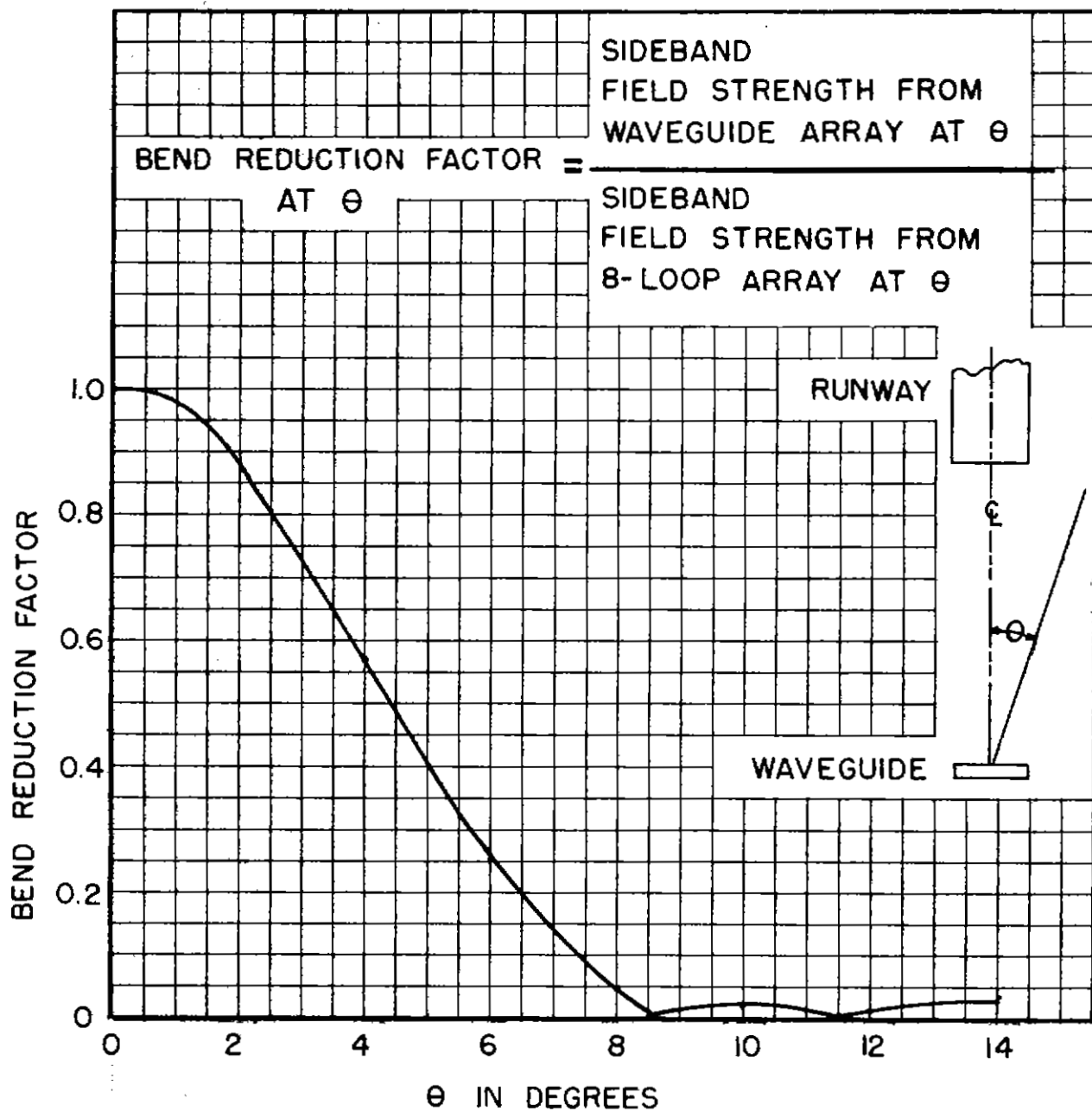


FIG. 18 BEND REDUCTION FACTOR OF 117-FOOT WAVEGUIDE

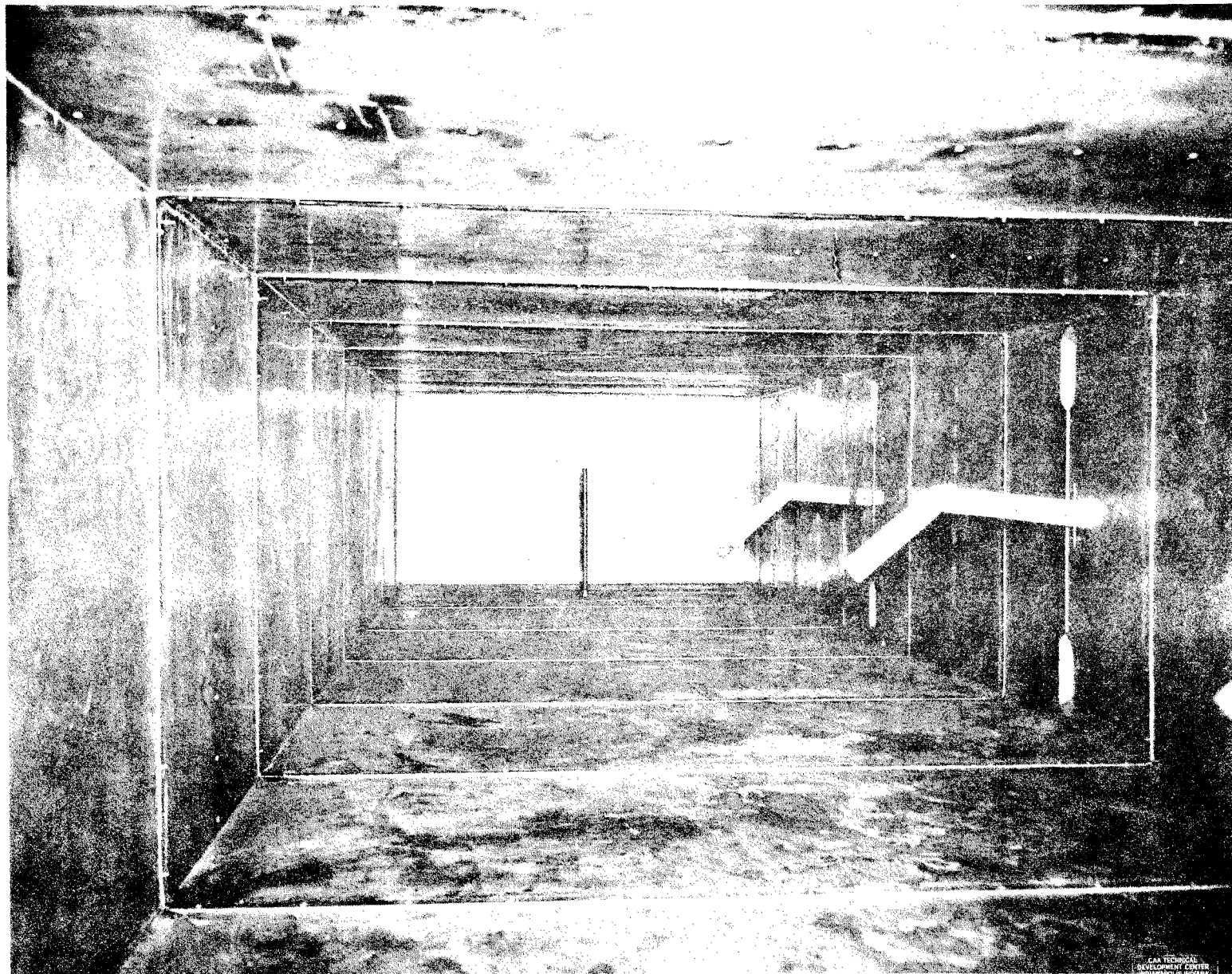


FIG. 19 INTERIOR VIEW OF END OF WAVEGUIDE SHOWING EXCITATION PROBES  
AND TWO SLOT PROBES

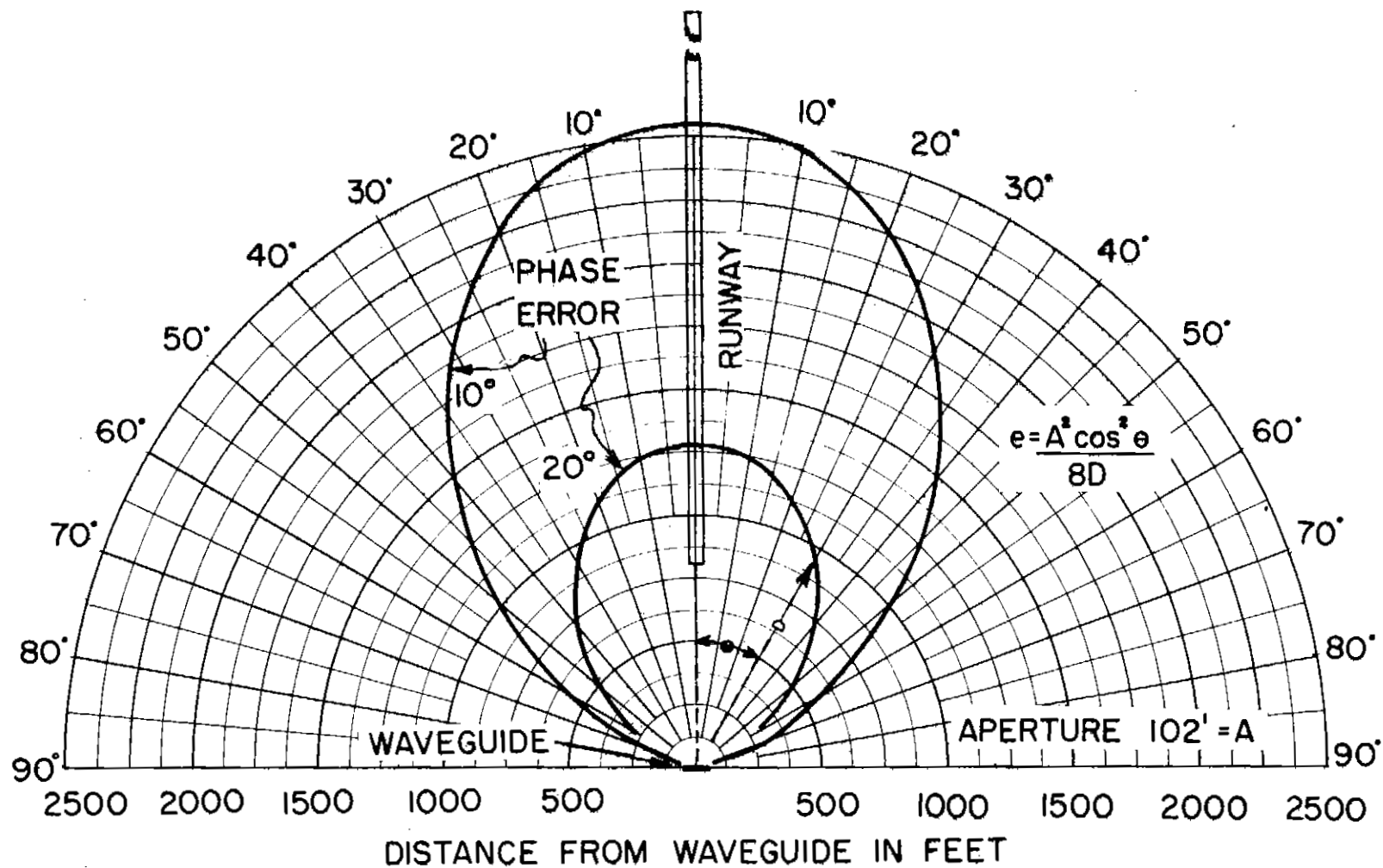


FIG. 20 PHASING ERROR BETWEEN END SLOTS AND CENTER OF WAVEGUIDE  
DUE TO PROXIMITY OF OBSERVER TO WAVEGUIDE

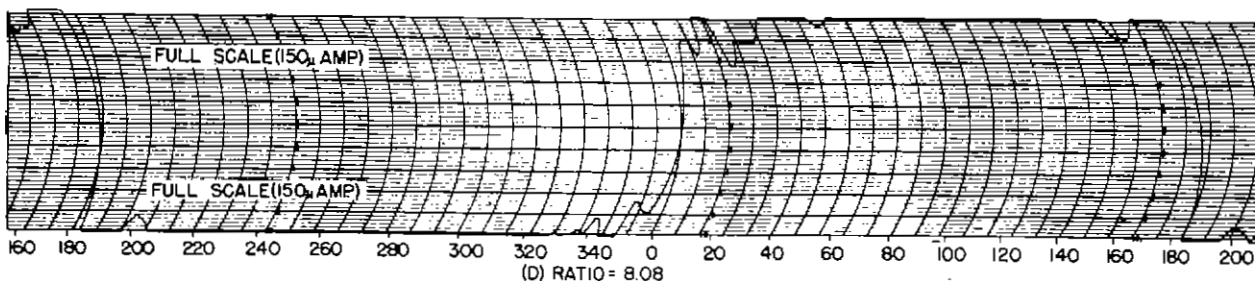
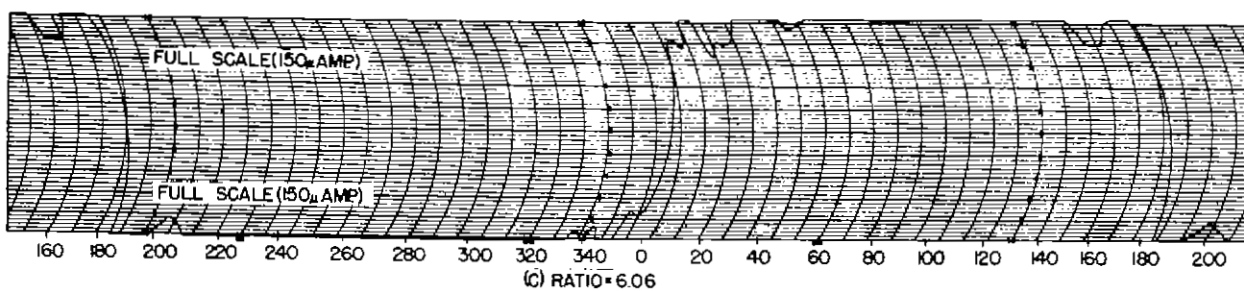
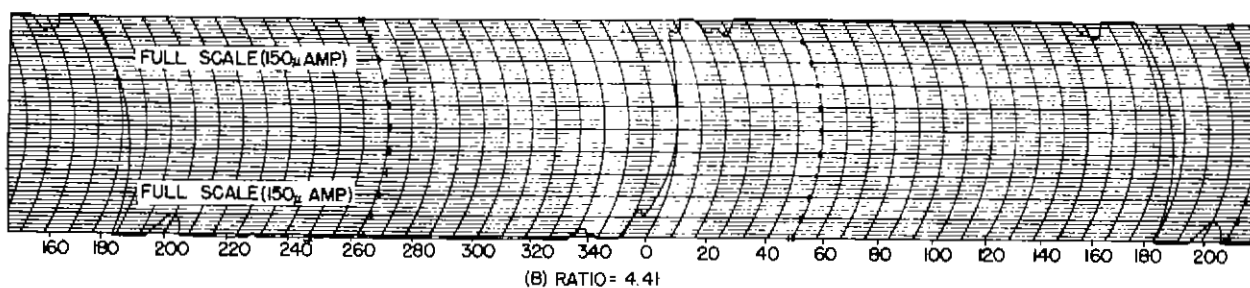
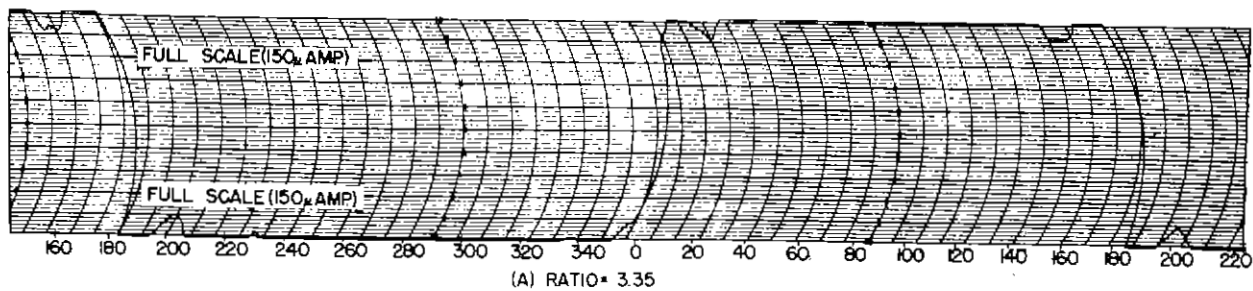
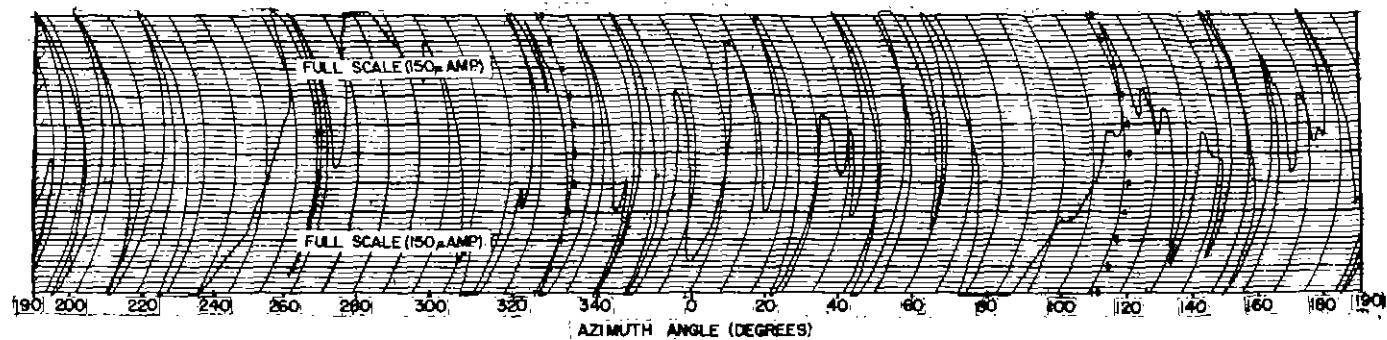


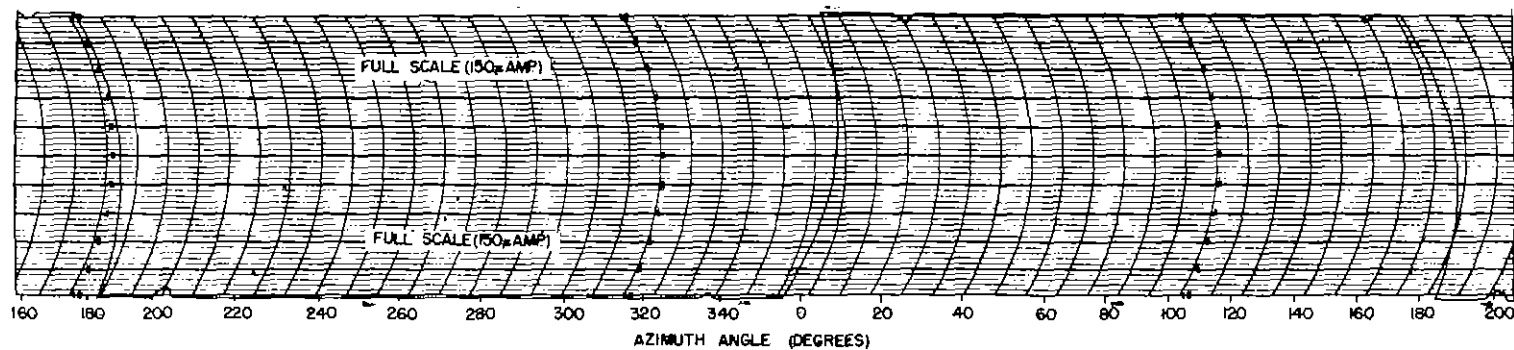
FIG. 21 EFFECT ON CDI CURRENT PRODUCED BY CHANGE IN RATIO OF FIELD STRENGTH OF WAVEGUIDE ARRAY TO FIELD STRENGTH OF CLEARANCE ARRAY.

FIG. 21 EFFECT ON CDI CURRENT OF CHANGING CLEARANCE ARRAY POWER

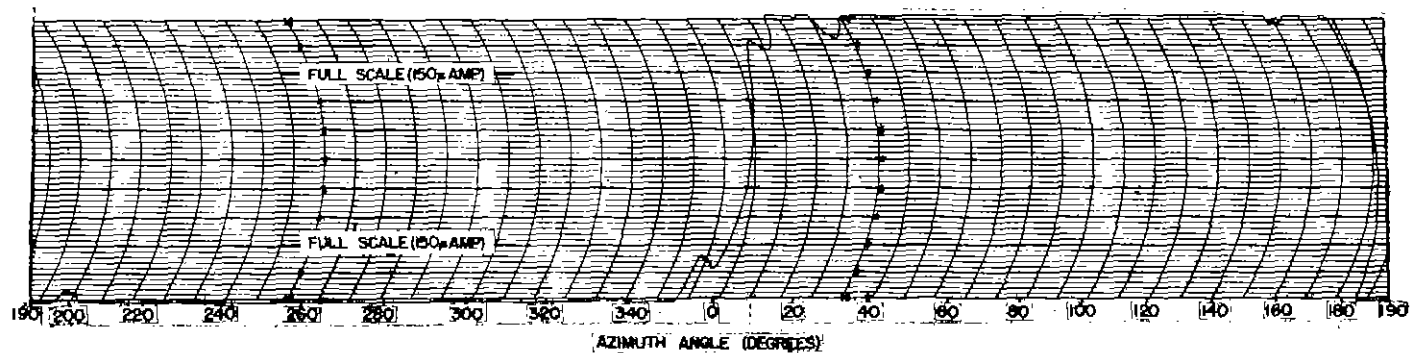




(A) WAVEGUIDE ARRAY



(B) CLEARANCE ARRAY



(C) COMBINED ARRAY

FIG 22 DIRECTIONAL LOCALIZER CDI RECORDINGS

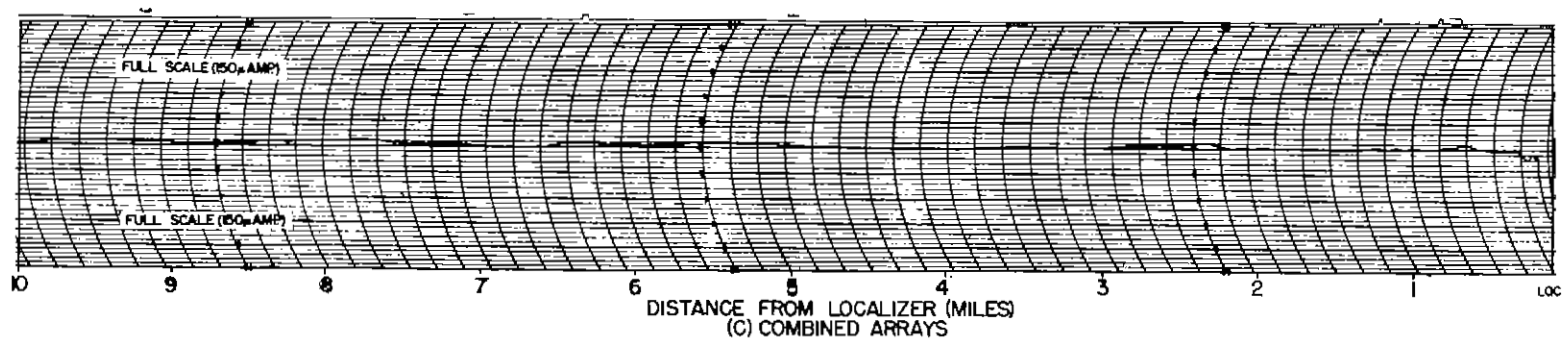
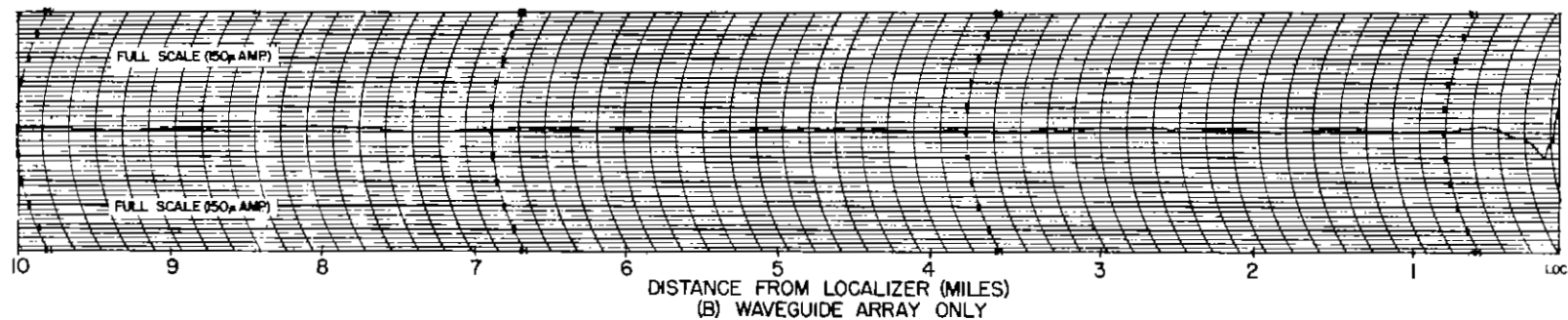
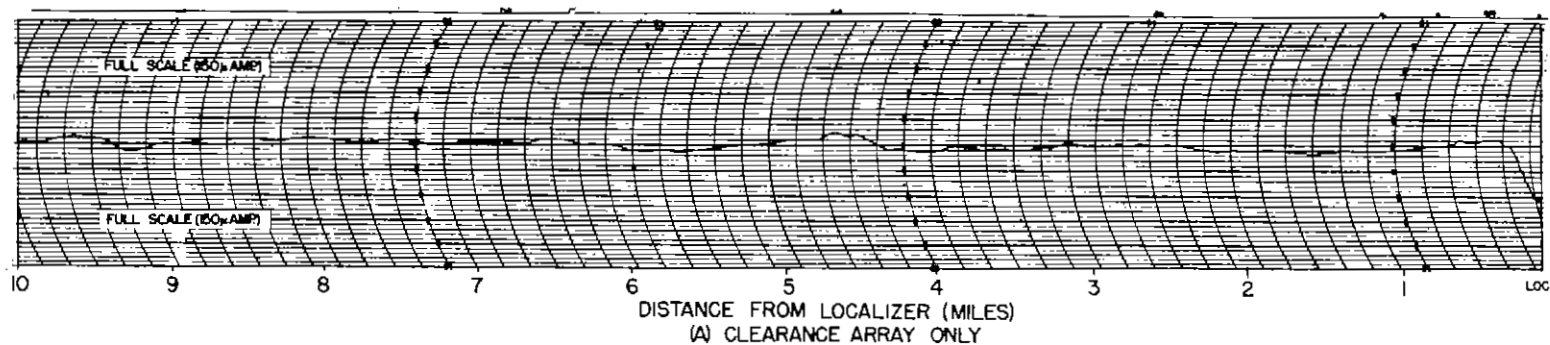


FIG 23 RECORDING OF CDI CURRENT  
DURING LOW APPROACH

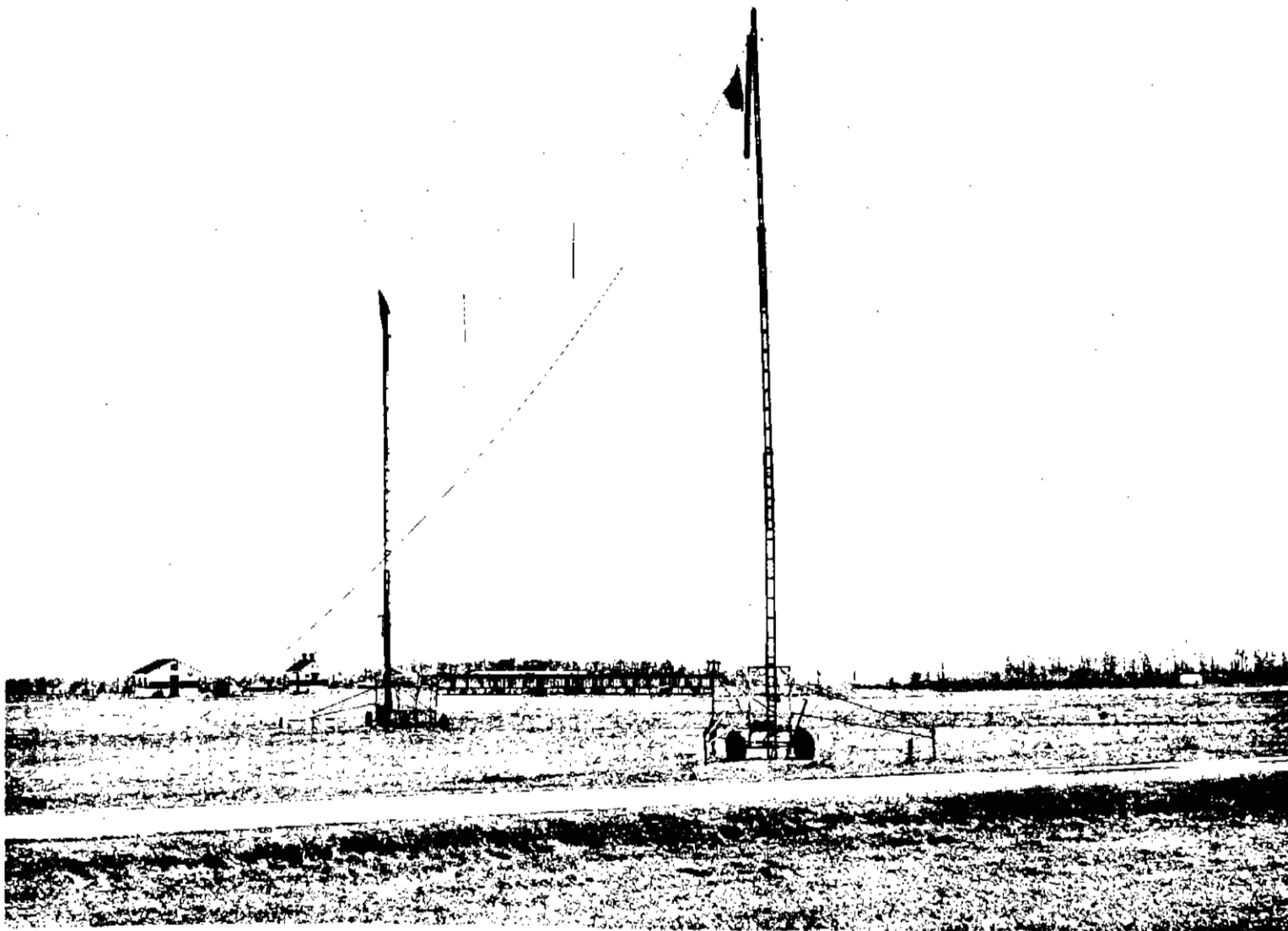


FIG. 24 VERTICAL SCREEN REFLECTOR POSITIONED IN FRONT OF ANTENNA SYSTEM

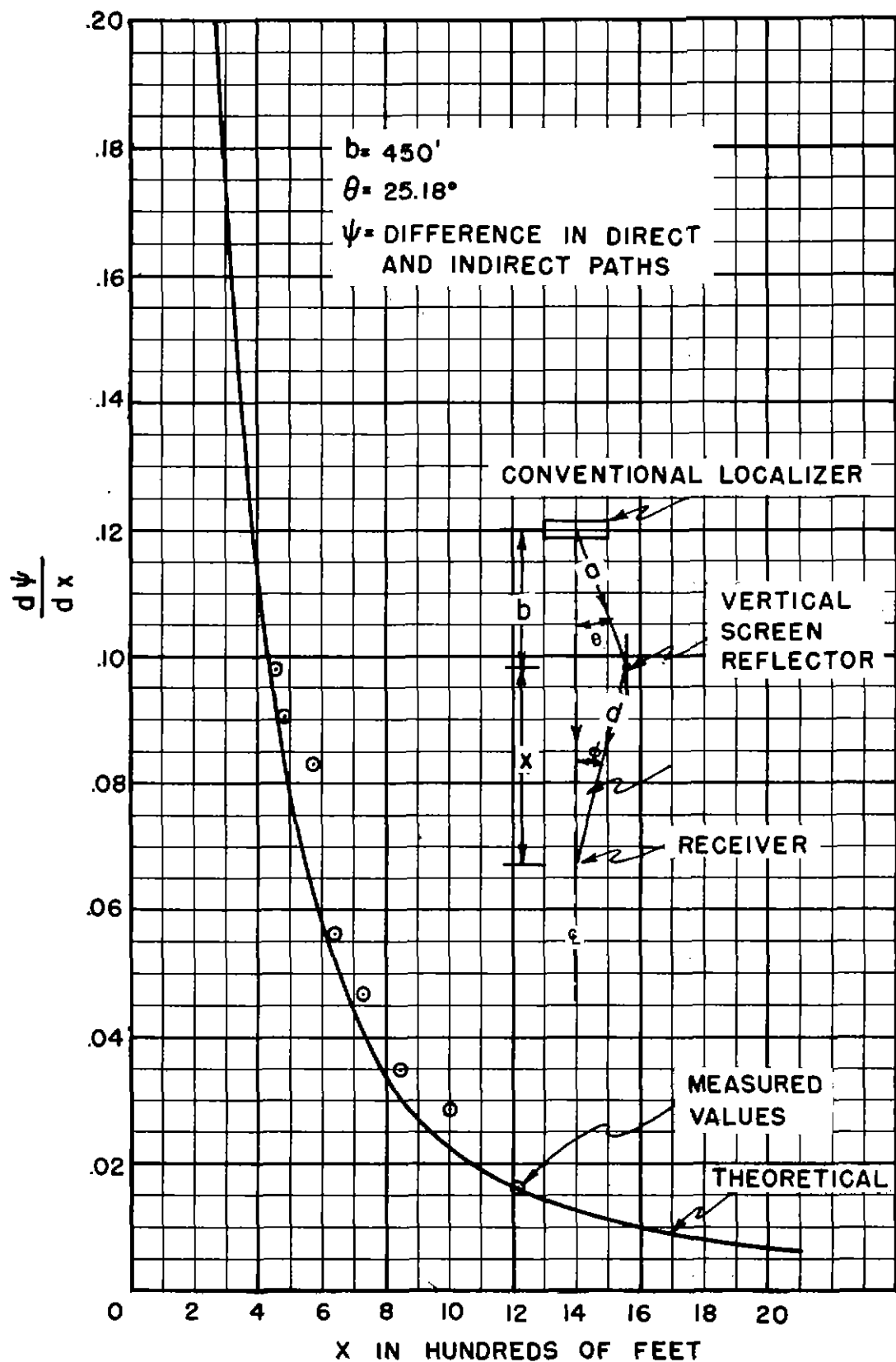


FIG. 25 THEORETICAL AND MEASURED CHANGE IN  $\psi$  WITH RESPECT TO DISTANCE FROM THE 8-LOOP ANTENNA ARRAY - VERTICAL SCREEN REFLECTOR POSITIONED PARALLEL TO THE COURSE

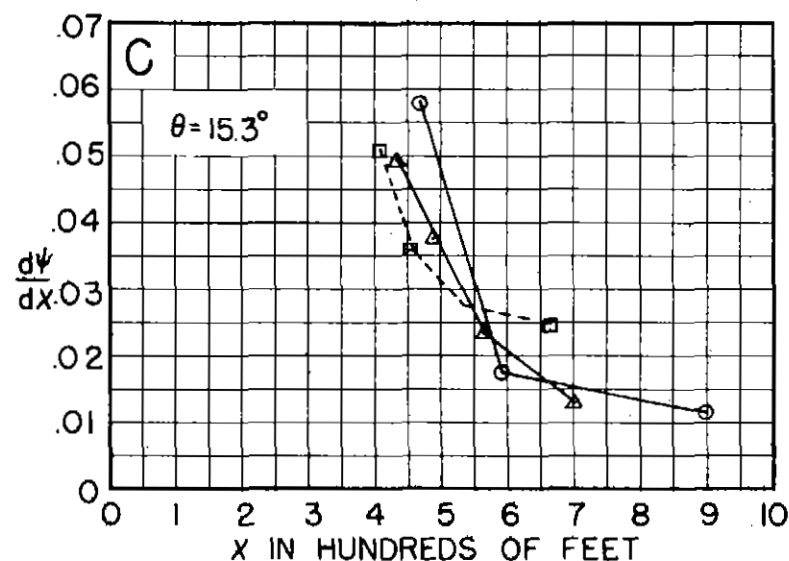
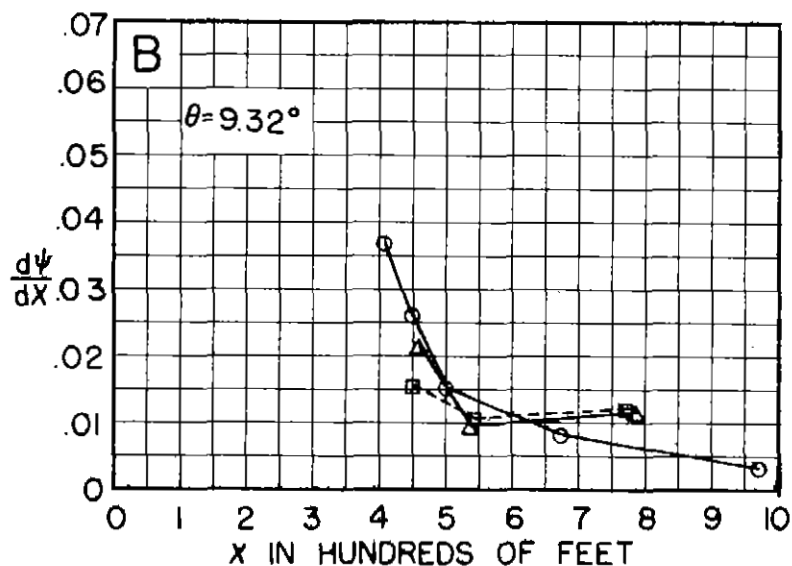
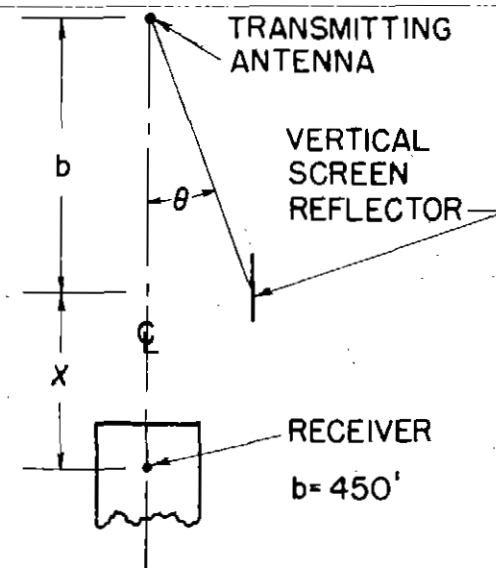
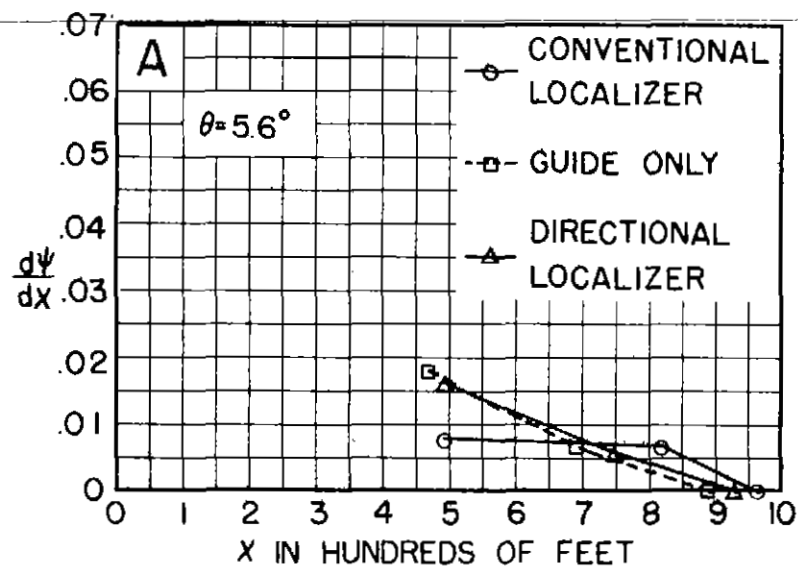


FIG. 26 MEASURED  $\frac{d\psi}{dx}$  WITH THE VERTICAL SCREEN REFLECTOR POSITIONED  
D  
AT VARIOUS VALUES OF  $\theta$  AND ORIENTED PARALLEL TO THE COURSE

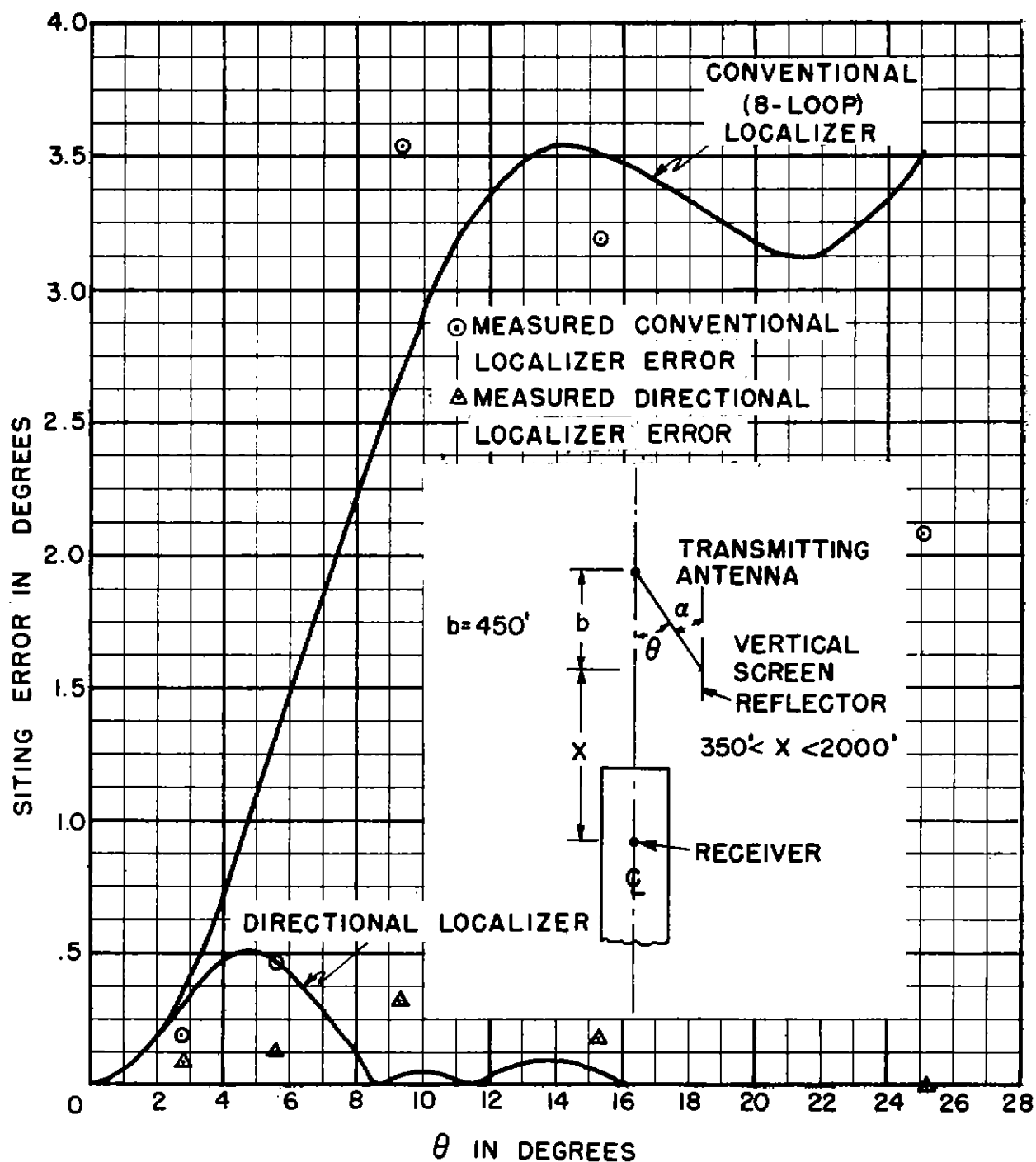


FIG. 27 THEORETICAL AND MEASURED SITING ERROR OF THE CONVENTIONAL AND DIRECTIONAL LOCALIZER CAUSED BY A VERTICAL SCREEN REFLECTOR POSITIONED PARALLEL TO THE COURSE

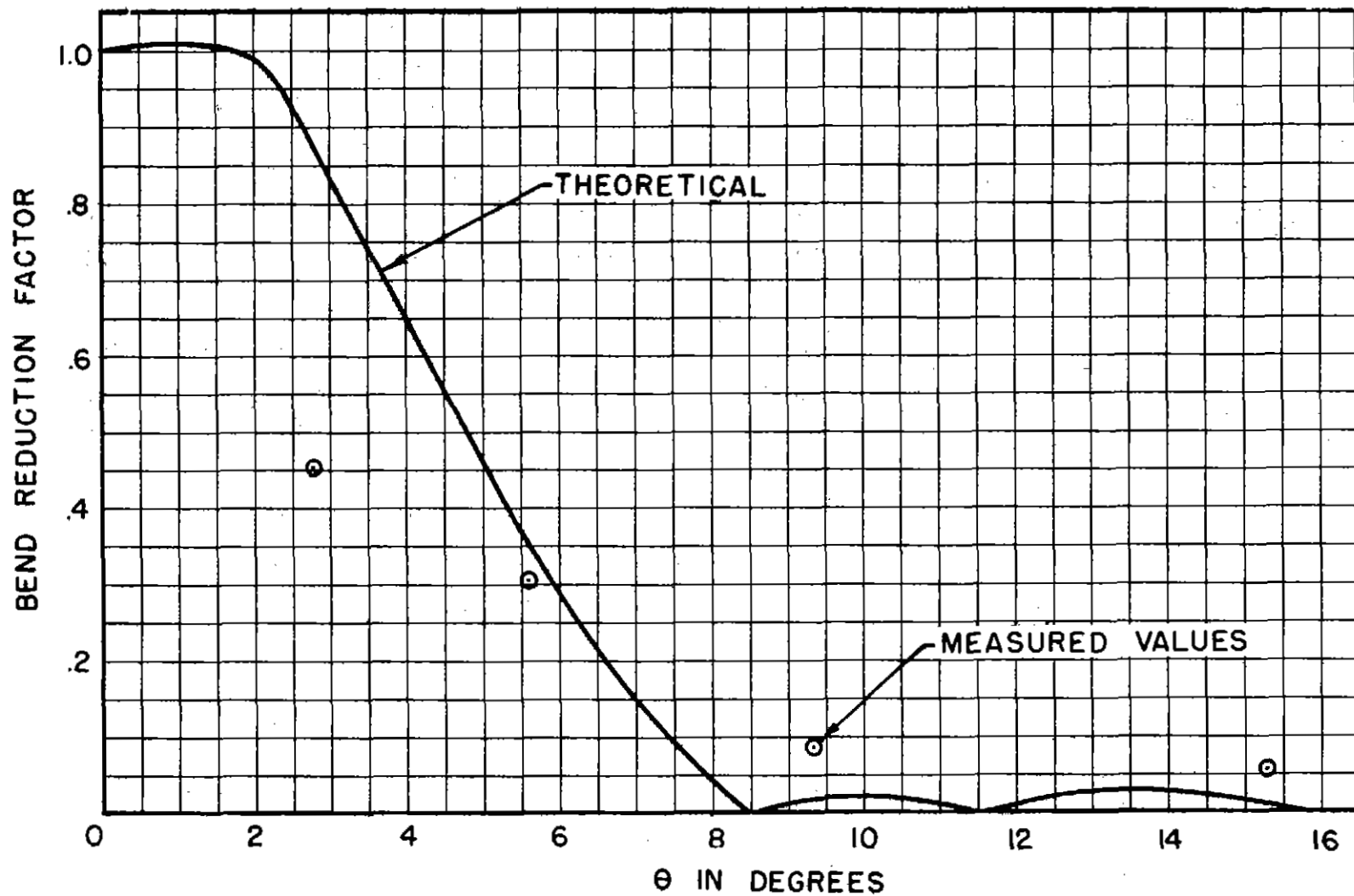


FIG. 28 BEND REDUCTION FACTOR FOR DIRECTIONAL LOCALIZER VERSUS CONVENTIONAL LOCALIZER OBTAINED WITH THE VERTICAL SCREEN REFLECTOR POSITIONED PARALLEL TO THE COURSE

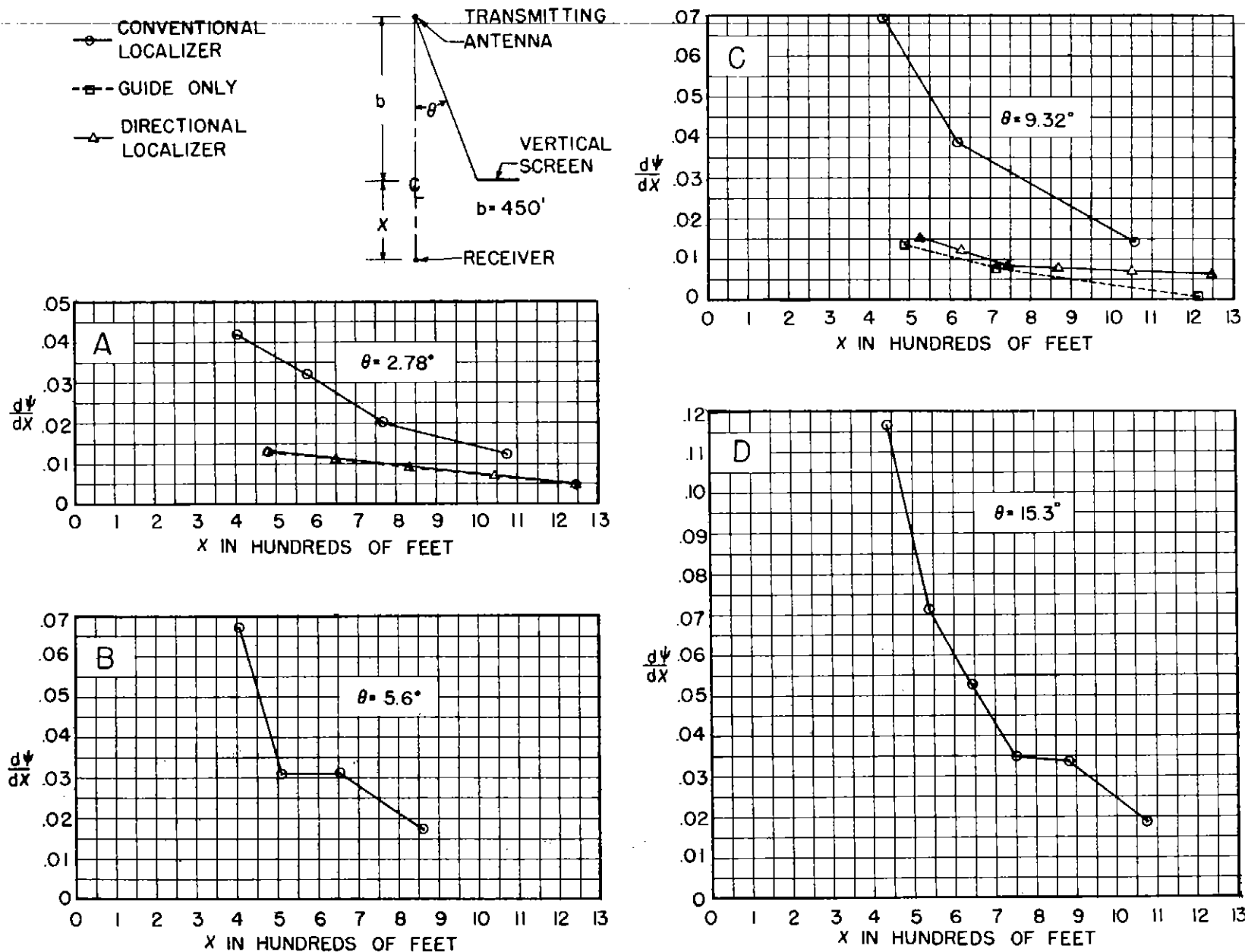


FIG. 29 MEASURED  $\frac{d\psi}{dx}$  WITH VERTICAL SCREEN POSITIONED AT VARIOUS VALUES OF  $\theta$  AND ORIENTED PERPENDICULAR TO THE COURSE



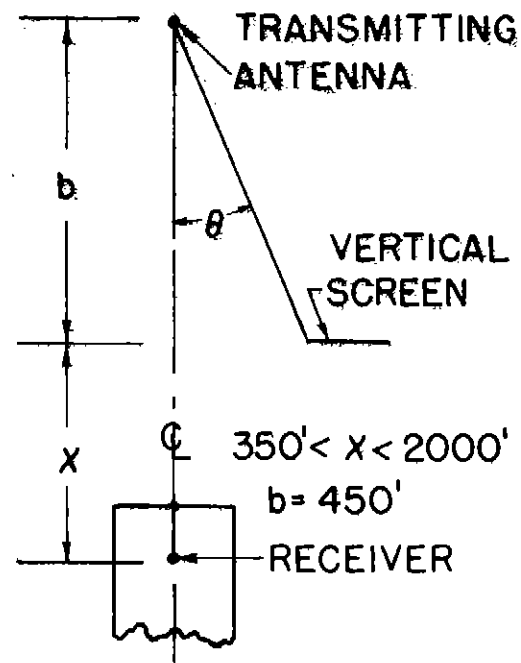
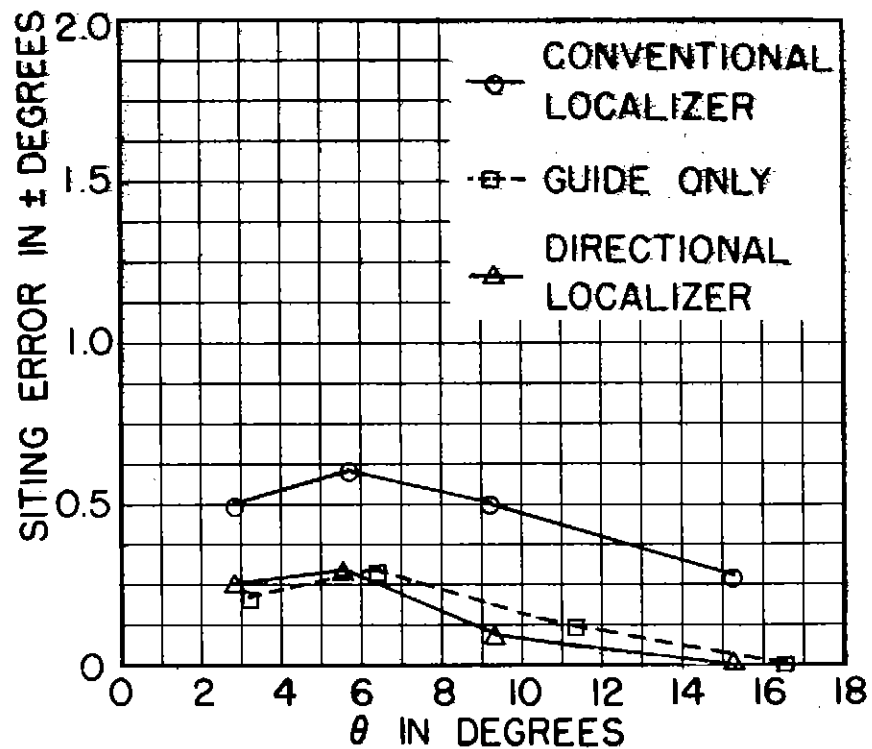


FIG. 30 MEASURED SITING ERROR CAUSED BY A VERTICAL SCREEN POSITIONED PERPENDICULAR TO THE COURSE

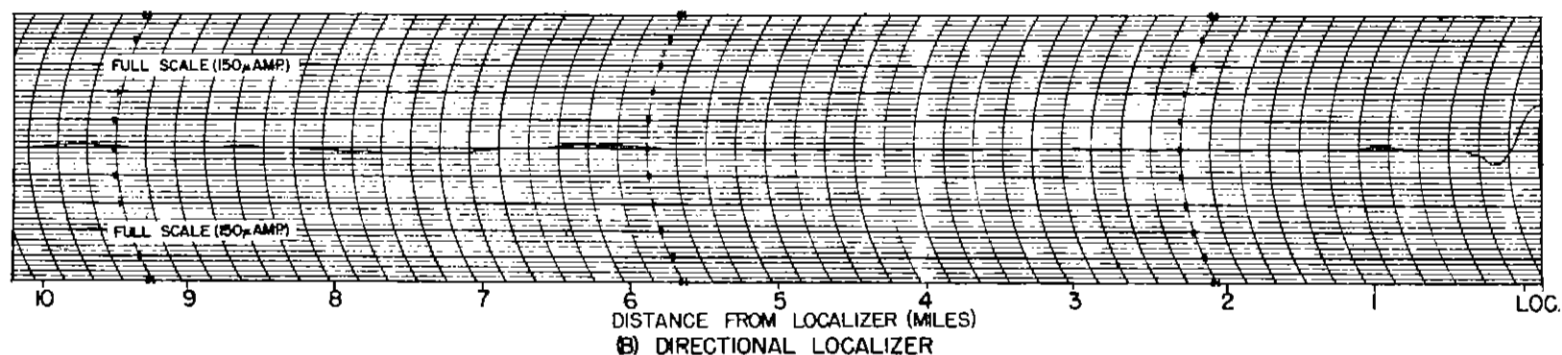
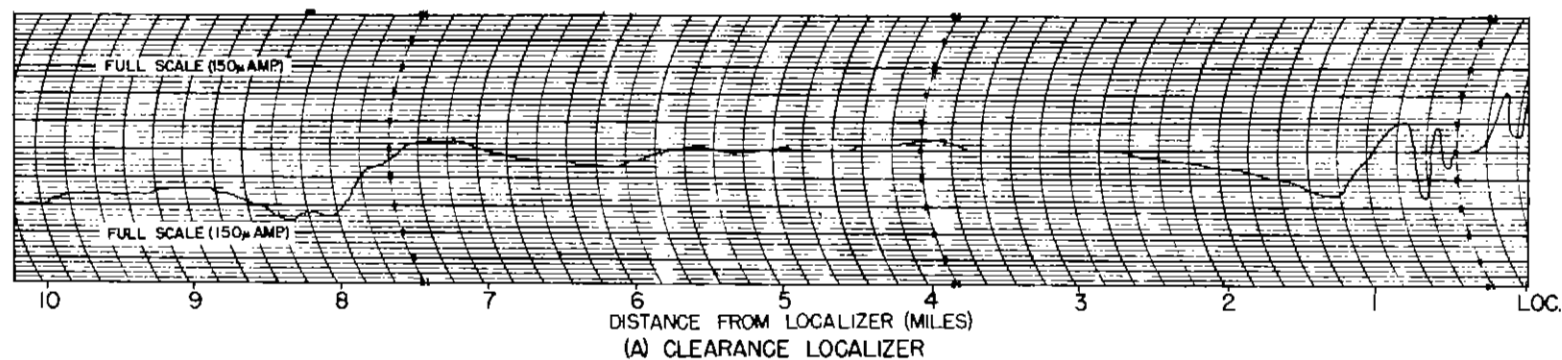
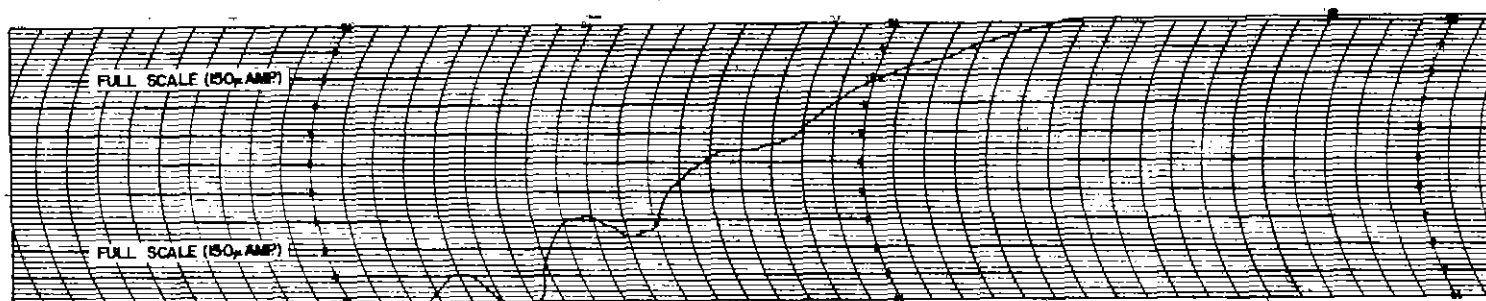
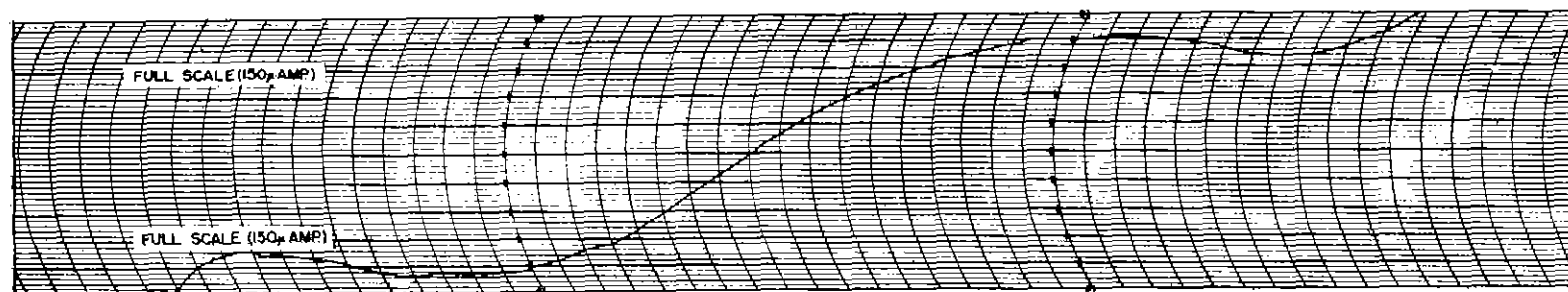


FIG 31 CDI RECORDINGS DURING LOW APPROACHES WITH VERTICAL SCREEN REFLECTOR POSITIONED IN FRONT OF ANTENNA SYSTEM

FIG. 31 CDI RECORDINGS DURING LOW APPROACHES WITH VERTICAL SCREEN REFLECTOR POSITIONED IN FRONT OF ANTENNA SYSTEM



(A) CLEARANCE LOCALIZER



(B) DIRECTIONAL LOCALIZER

FIG. 32 CDI RECORDINGS MADE WHILE FLYING ACROSS COURSE WITH VERTICAL SCREEN REFLECTOR POSITIONED IN FRONT OF ANTENNA SYSTEM

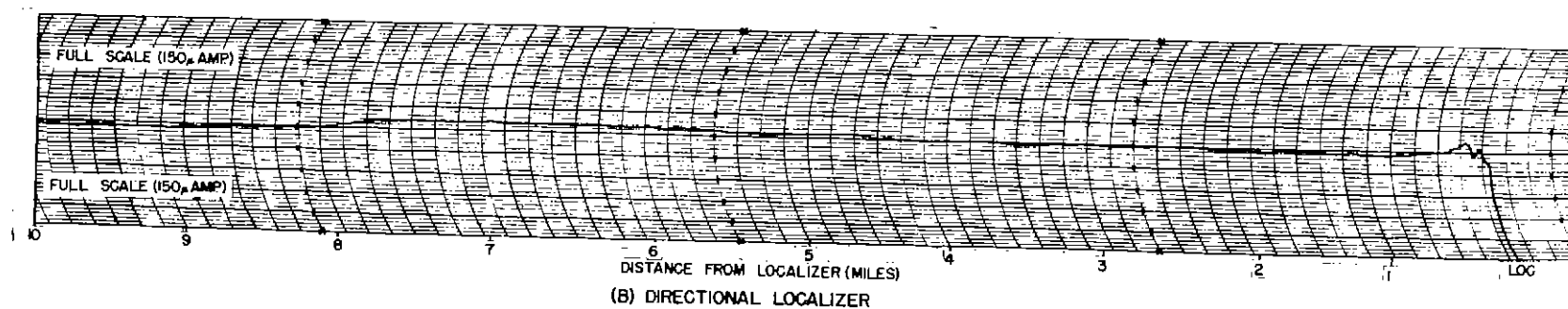
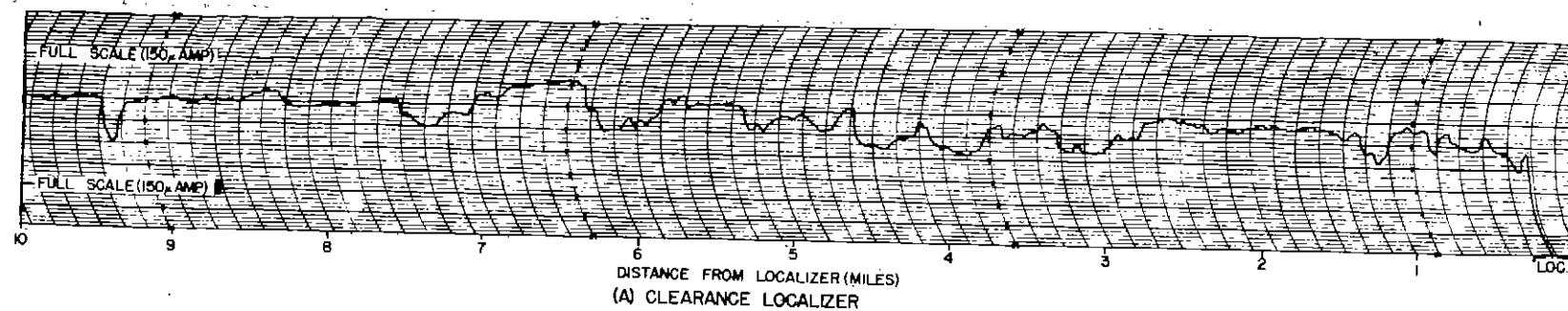
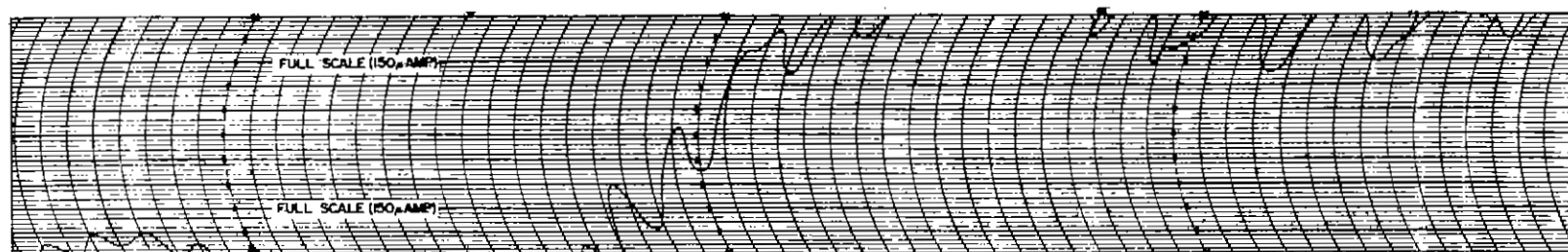
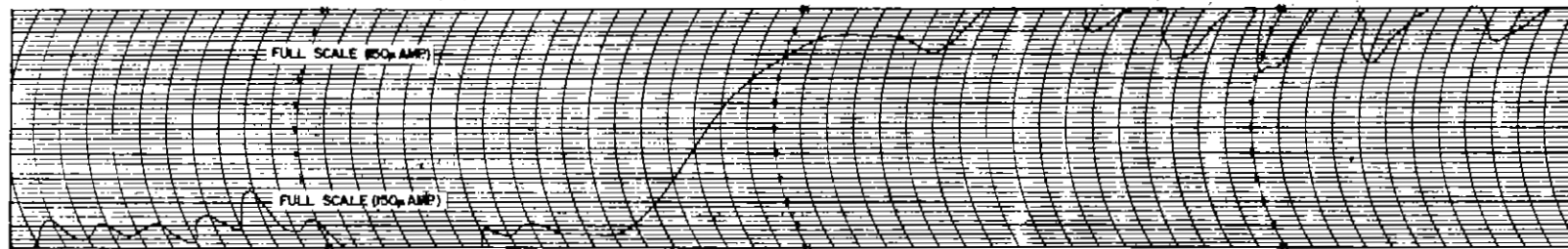


FIG. 33 CDI RECORDINGS DURING LOW APPROACHES WITH VERTICAL SCREEN REFLECTOR POSITIONED IN BACK OF ANTENNA SYSTEM



(A) CLEARANCE LOCALIZER



(B) DIRECTIONAL LOCALIZER

FIG. 34 CDI RECORDINGS MADE WHILE FLYING ACROSS COURSE WITH VERTICAL SCREEN REFLECTOR POSITIONED IN BACK OF ANTENNA SYSTEM

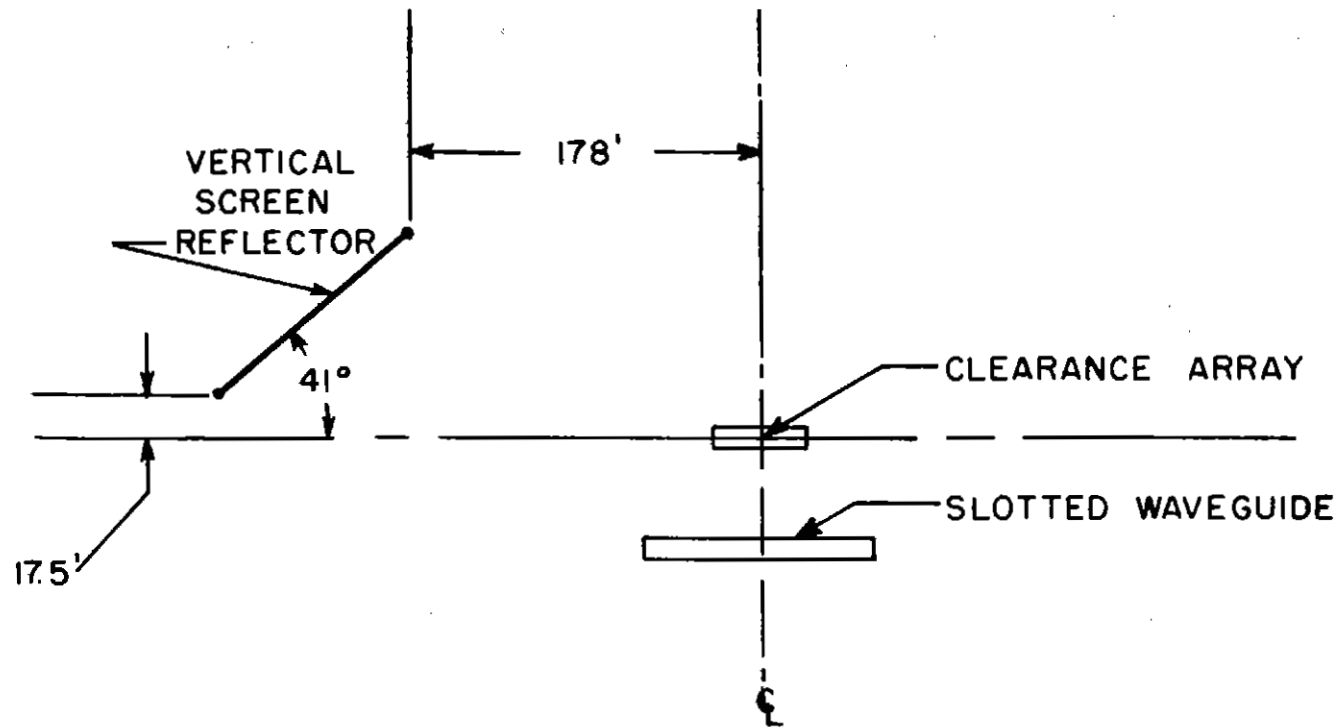


FIG. 35 RELATIVE POSITION OF VERTICAL SCREEN AS USED IN SITING TESTS

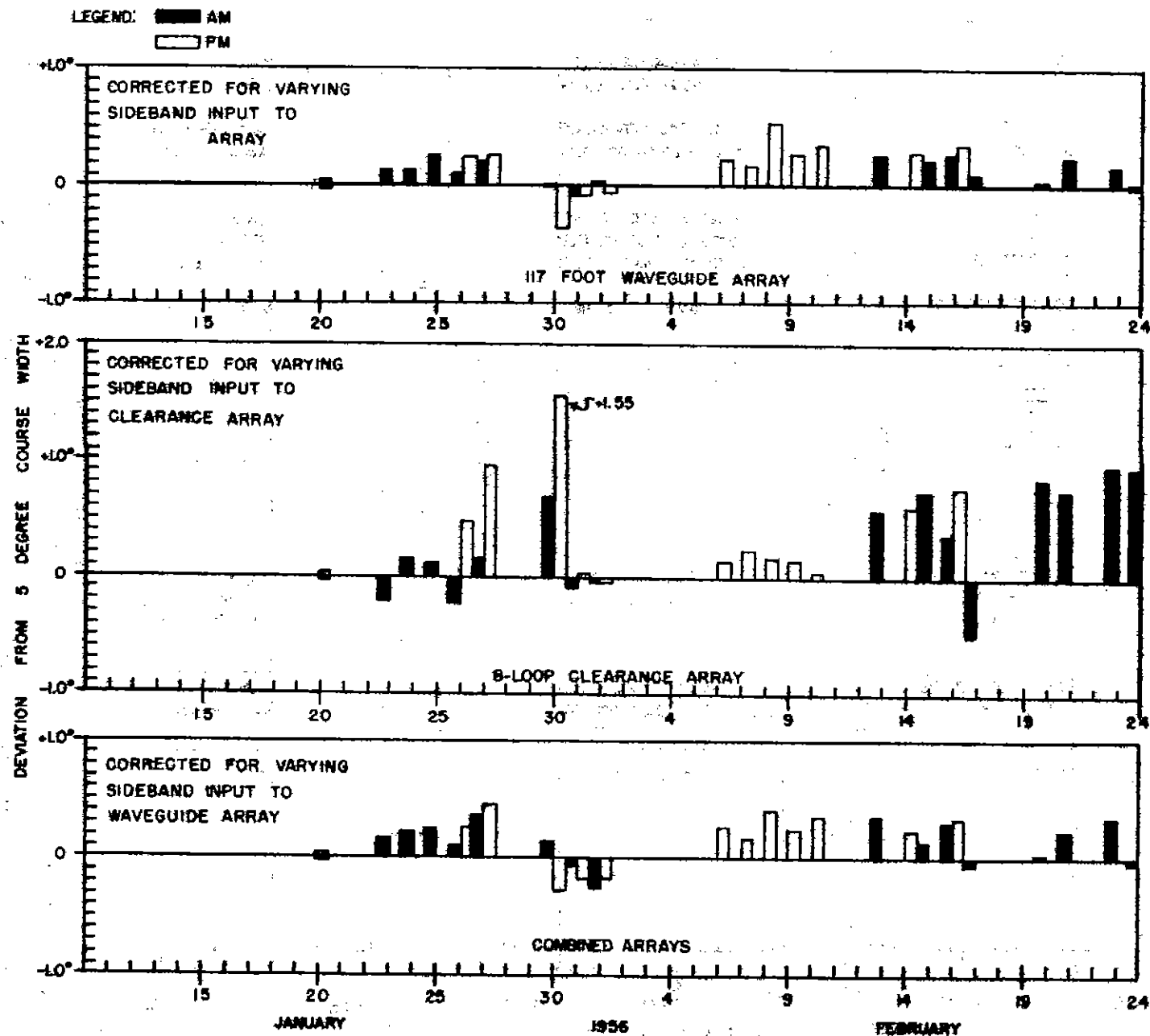


FIG. 36 COURSE WIDTH VARIATION - DIRECTIONAL LOCALIZER WITH 117-FOOT WAVEGUIDE

LEGEND:

■ A.M.  
□ P.M.

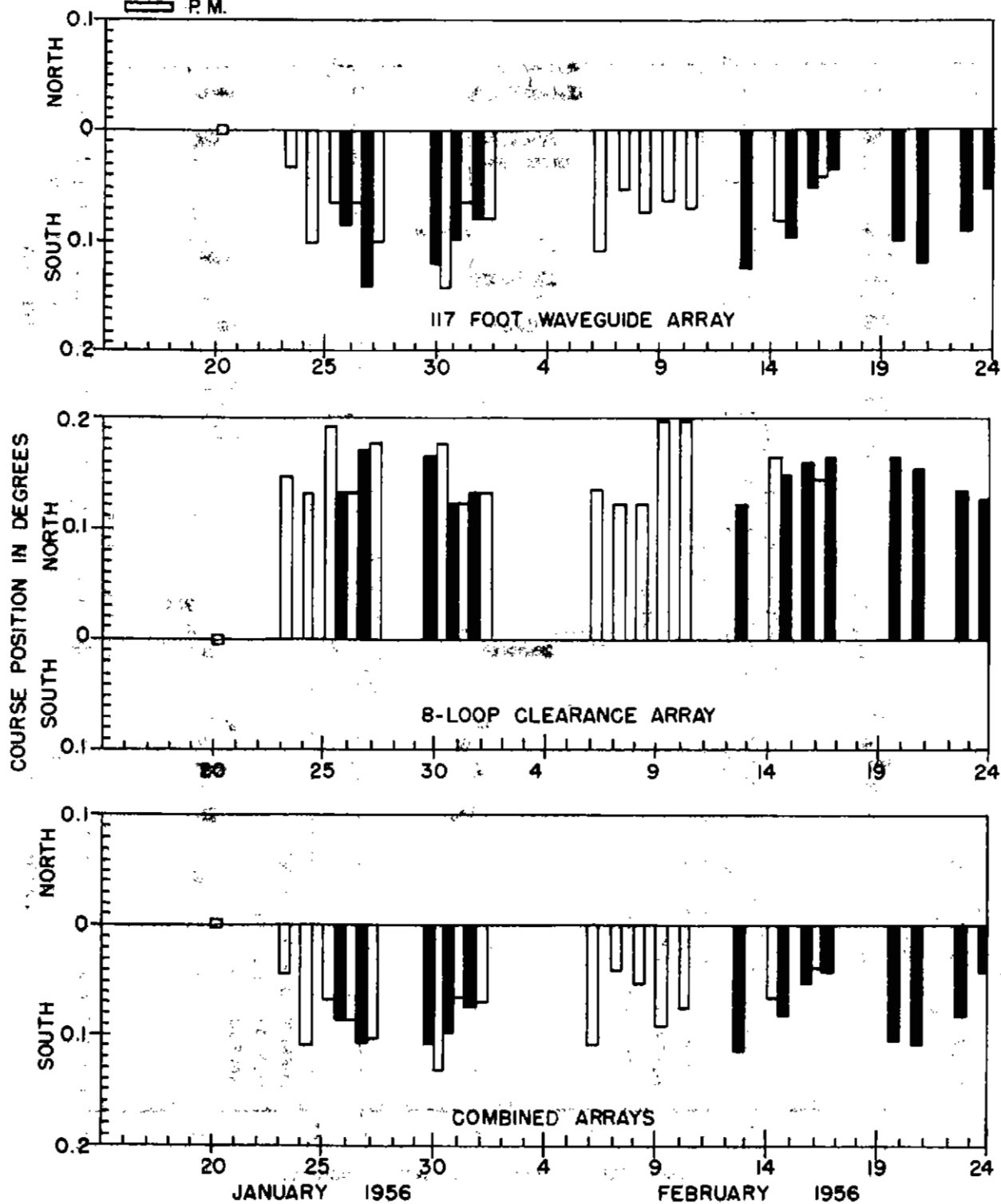


FIG. 37 COURSE POSITION VARIATION OF DIRECTIONAL LOCALIZER USING 117-FOOT WAVEGUIDE